



**CHALMERS**  
UNIVERSITY OF TECHNOLOGY



# CO<sub>2</sub> Reduction Measures in Steam Cracker Plants

Process integration opportunities of electrified steam methane reforming for fuel gas valorization

Master's thesis in Sustainable Energy Systems

Tobias Lehle

---

DEPARTMENT OF Space, Earth and Environment  
CHALMERS UNIVERSITY OF TECHNOLOGY  
Gothenburg, Sweden 2022  
[www.chalmers.se](http://www.chalmers.se)



MASTER'S THESIS 2022

# CO<sub>2</sub> Reduction Measures in Steam Cracker Plants

Process integration opportunities of electrified steam methane  
reforming for fuel gas valorization

TOBIAS LEHLE



**CHALMERS**  
UNIVERSITY OF TECHNOLOGY

DEPARTMENT OF Space, Earth and Environment  
*Division of Energy Technology*  
CHALMERS UNIVERSITY OF TECHNOLOGY  
Gothenburg, Sweden 2022

CO<sub>2</sub> Reduction Measures in Steam Cracker Plants  
Process integration opportunities of electrified steam methane reforming for fuel gas  
valorization  
Tobias Lehle

© Tobias Lehle, 2022.

Supervisor: Tharun Roshan Kumar, Department of Space, Earth and Environment  
Supervisor: Simon Harvey, Department of Space, Earth and Environment  
Examiner: Henrik Thunman, Department of Space, Earth and Environment

Master's Thesis 2022  
Department of Space, Earth and Environment  
Division of Energy Technology  
Chalmers University of Technology  
SE-412 96 Gothenburg  
Telephone +46 31 772 1000

Cover: Steam Cracker Furnace [1]

Typeset in L<sup>A</sup>T<sub>E</sub>X  
Printed by Chalmers Reproservice  
Gothenburg, Sweden 2022

## CO<sub>2</sub> Reduction Measures in Steam Cracker Plants

Process integration opportunities of electrified steam methane reforming for fuel gas valorization

Tobias Lehle

Department of Space, Earth and Environment

*Division of Energy Technology*

Chalmers University of Technology

## Abstract

Steam cracking is the main production route for the light olefins ethylene and propylene, which are considered a cornerstone of the chemical industry. The endothermic cracking reactions are conventionally supplied with heat by combusting fossil fuel and therefore entail large carbon dioxide emissions. Typically the fuel grade byproducts methane and hydrogen are used as fuel gas. Possible options to decarbonize the process include either the substitution of fossil feedstock, by e.g. biomass or recycled waste, or the heat supply to the reactions. While the industry strives for electrification of the cracker to decarbonize the heat supply, using hydrogen as fuel gas is a readily available decarbonization measure. To obtain hydrogen, the co-produced methane can be reformed. This work modelled the integration of an electrified steam methane reformer with an ethane steam cracker. The emission reduction potential and impact on the energy balance of an ethane cracker of two emission reduction scenarios was analysed. One scenario is categorized as pre-combustion carbon capture, while the other uses oxy-fuel combustion to reduce emissions. It was shown that both scenarios allow significant emission reduction of approximately 95 %, where the residual emissions stem from electricity consumption assuming Sweden's carbon grid intensity. The modeled scenarios showed that usage of reformed hydrogen for combustion entails a lower increase ( $1.1 \text{ MJ/kg}_{\text{Ethylene}}$ ) in specific energy consumption than oxy-fuel combustion ( $1.7\text{-}2.4 \text{ MJ/kg}_{\text{Ethylene}}$ ).

Keywords: Steam Cracking, CO<sub>2</sub> Reduction, Steam Reformation, e-SMR, Methane Valorization, Fuel Switching, Pre-combustion, Oxy-fuel Combustion



# Acknowledgements

I want to thank everybody who made this thesis possible. The fellow students I met in my two years in the Nordics, and the colleagues in the Energy Technology division of the Department of Space, Earth and Environment, which all made studying more fun and helped me learn a lot. Thanks to the friends I made abroad and of course my family and friends back home, which always supported me in the more stressful times of this Master program. Thanks to Tharun Kumar for his patience and academic guidance during this thesis. Thanks to Simon Harvey for the constructive feedback and thanks to Lars Pettersson for the insights into the details and challenges of cracker plant operation.

Thanks to all of you

Tobias Lehle, Gothenburg, June 2022



# List of Acronyms

Below is the list of acronyms that have been used throughout this thesis listed in alphabetical order:

ASU	Air Separation Unit
e-SMR	electrified Steam Methane Reforming
MTO	Methanol-to-Olefins
MEA	Monoethanolamine
NSG	Net Specific Steam Generation
PSA	Pressure Swing Adsorption
SE	Specific Emissions
SEC	Specific Energy Consumption
SFG	Specific Fuel Gas Consumption
SMR	Steam Methane Reforming
TLE	Transfer Line Exchanger
WGS	Water Gas Shift



# Contents

<b>List of Acronyms</b>	<b>ix</b>
<b>List of Figures</b>	<b>xiii</b>
<b>List of Tables</b>	<b>xv</b>
<b>1 Introduction</b>	<b>1</b>
1.1 Objectives . . . . .	2
<b>2 Theory</b>	<b>3</b>
2.1 Steam Cracking . . . . .	3
2.2 Carbon Capture . . . . .	5
2.3 Carbon Utilization . . . . .	6
2.4 Electrified Steam Methane Reforming . . . . .	6
<b>3 Methods</b>	<b>9</b>
3.1 Scenario Selection . . . . .	10
3.2 System Boundary . . . . .	10
3.3 Performance Indicators . . . . .	13
<b>4 Process Modeling</b>	<b>15</b>
4.1 Cracker Furnace . . . . .	15
4.1.1 Model Description . . . . .	15
4.1.2 Control System . . . . .	17
4.1.3 Validation . . . . .	18
4.2 Reformer . . . . .	19
4.2.1 Model Description . . . . .	19
4.2.2 Validation . . . . .	20
<b>5 Results and Discussion</b>	<b>21</b>
5.1 Hydrogen Firing . . . . .	21
5.2 Oxyfuel . . . . .	22
5.3 Comparison of the Scenarios . . . . .	24
5.4 Carbon Utilization . . . . .	29
5.5 Discussion . . . . .	29
<b>6 Conclusion</b>	<b>31</b>

6.1	Limitations and Suggestions for Future Work . . . . .	32
	<b>Bibliography</b>	<b>33</b>
A		I
B		III
C		V
D		VII

# List of Figures

3.1	Methodological approach . . . . .	9
3.2	System Boundary of a conventional cracker furnace . . . . .	10
3.3	System Boundary for the <i>Hydrogen Firing</i> scenario . . . . .	11
3.4	System Boundary for the <i>Oxyfuel</i> scenario . . . . .	12
4.1	Convection section of the modeled cracker furnace . . . . .	16
4.2	Flowsheet of the reformer model . . . . .	19
5.1	Specific energy consumption and net steam generation of the investigated scenarios . . . . .	24
5.2	Specific uncaptured emissions associated with the investigated scenarios compared to a conventional cracker (solid line) and a conventional cracker with post-combustion CO <sub>2</sub> capture (ellipse), plotted against the additional specific energy consumption required for emission reduction . . . . .	25
5.3	Specific uncaptured emissions associated with the investigated scenarios compared to a conventional cracker (solid line) and a conventional cracker with post-combustion CO <sub>2</sub> capture (ellipse), plotted against the additional specific energy consumption required for emission reduction, excluding steam generation by a steam boiler . . . . .	26
5.4	Emission composition of the investigated scenarios . . . . .	27
5.5	Emission composition of the investigated scenarios excluding steam generation by a steam boiler . . . . .	28
A.1	Heat Integration for <i>Hydrogen Firing</i> scenario . . . . .	II
A.2	Heat Integration for <i>Oxyfuel</i> scenario . . . . .	II
D.1	System Boundary for <i>Oxyfuel V2</i> . . . . .	VII



# List of Tables

2.1	Cracked gas composition . . . . .	4
3.1	Overview of the KPIs . . . . .	14
4.1	Specified constraints for heat integration . . . . .	17
4.2	Parameters of the cracker model . . . . .	17
4.3	KPIs of the conventional cracker model, modified cracker model and literature values . . . . .	18
4.4	Parameters of the e-SMR model . . . . .	20
4.5	Validation e-SMR . . . . .	20
5.1	KPIs <i>Hydrogen Firing</i> . . . . .	21
5.2	Depleted syngas composition <i>Hydrogen Firing</i> . . . . .	22
5.3	KPIs <i>Oxyfuel</i> . . . . .	22
5.4	Shifted syngas composition <i>Oxyfuel</i> . . . . .	23
5.5	Flue gas composition <i>Oxyfuel</i> . . . . .	23
5.6	KPIs <i>Oxyfuel V2</i> . . . . .	23
A.1	Stream data for the <i>Hydrogen Firing</i> scenario . . . . .	I
A.2	Stream data for the <i>Oxyfuel</i> scenarios . . . . .	II



# 1

## Introduction

Polyethylene is the material from which most plastic products are made today, and is therefore present in many everyday products and parts of industrial value chains. Polyethylene is produced by polymerizing ethylene, the simplest derivative of the alkenes, a group of hydrocarbons characterized by their carbon-carbon double bond. In addition to polyethylene production, ethylene is also an important starting material for other products, such as polyester fibers and antifreeze agents, making it a cornerstone of the chemical industry [2].

The primary production route for ethylene is steam cracking, also referred to as thermal cracking. The process is characterized by high energy intensity, as elevated temperatures are required to break down the feedstock. This energy demand is conventionally supplied by combustion of fuel gas. While no detailed estimates are available, the global production capacity is on the order of magnitude of  $10^8$   $t/a$ , which in combination with reported specific emissions of 1-1.2  $t_{CO_2}/t_{Ethylene}$  for steam cracking makes ethylene production a significant global emitter of carbon dioxide [3][4].

The main decarbonization strategies for steam cracking can be categorized into three key areas. The first of these measures is to increase energy efficiency, which is generally considered to be already well exhausted in conventional steam crackers and therefore unlikely to contribute to significant emissions reductions [5]. Another area addresses the fossil feedstock, which can be replaced by bio-based or plastic waste feedstock [6]. Alternatively, the need for fossil feedstock can be reduced by chemical recycling of plastic waste to directly obtain polyolefins for plastic production [7][8]. The last key area concerns the provision of thermal energy for the cracking reactions. One approach is the direct electrification of the heat supply, preferably using renewable electricity. A consortium of several petrochemical companies pursues this approach in a joint effort, but has not announced a road map so far [6]. The other approaches, which are the main subject of this work, focus on reducing emissions when combustion of fuel is used to provide the thermal energy needed for cracking. In a recent publication *Mynko et al.* [9] conducted a life cycle assessment of several revamp strategies aiming to reduce  $CO_2$  emissions of steam crackers. Oxy-fuel combustion with further carbon capture and storage showed the greatest emission reduction potential, followed by combustion of biogas. However, the analyses did not include a pre-combustion strategy, which is based on combusting hydrogen in the cracker furnace, thereby achieving a  $CO_2$  free flue gas [5]. The conventional process for producing hydrogen is steam methane reforming (SMR), which entails high emissions, of approximately 9  $kg_{CO_2}/kg_{H_2}$ , as fuel gas is combusted to supply heat to the endothermic SMR reaction [10]. However, electrifying steam methane reforming

has been subject to increased research lately and is expected to be one of the first steps in the electrification of the chemical industry [10][11][12]. Electrified steam methane reforming is applicable for steam crackers, as methane is co-produced in steam cracking. Methane can be valorized to a hydrogen-rich synthesis gas, that is either burned to provide energy for cracking or can be utilized for other purposes. This work investigates the emission reduction potential of the novel approach of integrating an electrified steam methane reformer with an ethane steam cracker.

### 1.1 Objectives

The objective of this work is the investigation of the emission reduction potential of different integration scenarios for an electrified steam methane reformer at an ethane cracker plant and a subsequent analyses of the impact on the crackers energy balance. More specifically this includes:

- Development of a process model of an electrified steam reformer and an ethane cracker in Aspen Plus® software
- Integration of the reformer and cracker models in different scenarios
- Quantifying the emission reduction potential and evaluating thermochemical performance of the integration scenarios
- Stating the limitations of the conducted work and pointing towards main areas of interest for future research

# 2

## Theory

This chapter addresses the theory of the main processes discussed in this work, namely steam cracking, carbon capture and utilization processes applicable and electrified steam methane reforming.

### 2.1 Steam Cracking

Light olefins, especially ethylene and propylene, are considered a cornerstone within the chemical industry, as they are used in the production of many other chemicals, fibers and the most widely used plastic in the world, polyethylene [2][3][13].

The main production route for ethylene is steam cracking, also referred to as thermal cracking. The potential feedstocks for steam cracking are ethane, propane, naphtha and butane. Typically, several cracker furnaces running on potentially different feedstock are located in a cracker plant. Often clusters form around these cracker plants, since they produce several useful by-products. Light olefins are produced by breaking down the saturated hydrocarbon chains of the feedstock in the steam cracking process, in which a multitude of co-products is generated. Steam cracking summarizes several endothermic cracking reactions which take place in the absence of oxygen. This endothermic conversion occurs in tubular reactors, which are heated by burning fuel gas in a furnace. Steam is added to dilute the feedstock and thereby reduce its partial pressure. This helps to steer the reaction towards formation of light olefins and inhibits unwanted secondary reactions. Dilution steam also helps to reduce coke formation on the inner reactor surfaces, as steam reacts with coke to form carbon monoxide, carbon dioxide, and hydrogen [14]. Typical ratios of steam to hydrocarbon feedstock are in the range 0.25-0.35 for ethane cracking [13].

Table 2.1 shows a typical dry gas compositions of the cracked gases from an ethane cracker.

**Table 2.1:** Cracked gas composition

Component	mol % [13]
Ethylene	35.41
Ethane	21.15
Hydrogen	38.23
Methane	3.29
Propylene	0.43
Propane	0.05
Acetylene	0.53
Butadiene	0.57
Butane	0.07
C <sub>5+</sub>	0.27

The main product of ethane cracking is ethylene, but the methane and hydrogen fractions are of special interest in this work. The yield of these two compounds is significantly higher for steam cracking of other feedstock such as naphtha and propane. However, there are several other valuable chemicals produced in steam cracking such as propylene, acetylene, butadiene and butane. As can be seen in the cracked gas composition there is also a significant amount of unreacted ethane. This fraction is typically recycled to the furnace to increase product yield [4].

The cracked gas needs to be rapidly cooled down to prevent degradation by further reactions. This is typically done in a Transfer Line Exchanger (TLE), where the sensible heat of the cracked gas is recovered by heat exchanging it against pressurized water that is heated and evaporated to generate steam [4].

The cracked gas needs further processing after the quenching in the TLE to obtain purified product streams. This is conducted in several distillation and fractionation steps [13].

The fuel-grade byproducts H<sub>2</sub> and CH<sub>4</sub> play a significant role in steam cracking plants as they are often used as fuel gas in the cracker furnace. However, a feature of ethane cracking is that the yield of these fuel-grade byproducts does typically not provide sufficient thermal energy required for cracking if combusted [4]. Therefore, additional fuel gas must be added, coming either from other cracking furnaces or supplied externally.

The furnace consists of two main parts, the radiation section, also referred to as the firebox, and the convection section with the stack. The radiation section hosts burners for fuel gas combustion while the reactor tubes are suspended in the combustion flame. The hot flue gas leaving the radiation section is subject to several heat integration steps in the convection section to recover its thermal energy. In this way, the feedstock is preheated to temperatures of 500-680 °C before entering the reactor tubes [13]. Furthermore, the flue gas contains enough thermal energy to also preheat water and superheat steam as part of the steam generation cycle with the TLE. This steam is typically used to drive compressors and refrigeration cycles, which are an essential part of the fractionation section of a cracker plant [6][15]. Many cracker plants have a steam boiler on site to ensure availability of steam, which is needed to dilute the feedstock and power the fractionation section.

## 2.2 Carbon Capture

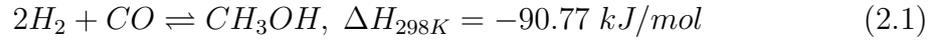
The three main approaches to capturing CO<sub>2</sub> emissions from cracker furnaces reported in literature are post-combustion capture, pre-combustion capture and oxy-fuel combustion [5]. Post-combustion capture aims at separating CO<sub>2</sub> from the flue gas of conventional combustion of hydrocarbons, which can be done with several methods. Membranes, cryogenic distillation, adsorption and chemical absorption are the main mechanism studied. Among these, chemical adsorption is the most common [6]. Flue gas is exposed to an adsorbent, which forms weak bonds with the CO<sub>2</sub> at low temperatures. The CO<sub>2</sub> can be released again by breaking this bond at higher temperatures in a reactor, referred to as desorber or stripper. The adsorbent can then be used for the same process again, but is subject to some degradation. The most frequently used organic solvent is monoethanolamine [16]. Typical capture rates are around 85-95 %, consequently leaving behind 15-5 % of the CO<sub>2</sub> in the flue gas uncaptured. The energy consumption for regeneration of the absorbent can range from 3-5 MJ/kg<sub>CO<sub>2</sub></sub> at temperatures of around 120 °C, which means that steam can be used as energy carrier for the regeneration of the adsorbent. Carbon capture by these means can be regarded as a retrofit solution with few changes to the cracking furnace, if low pressure steam for regeneration of the solvent is available [5].

Pre-combustion carbon sequestration is based on a fundamentally different approach, as it aims to separate CO<sub>2</sub> from the fuel before combustion. This often includes gasification of fossil or bio based fuels, to obtain synthesis gas, consisting primarily of H<sub>2</sub> and CO. The synthesis gas is processed further, converting CO and steam to H<sub>2</sub> and CO<sub>2</sub>, according to the WGS Reaction 2.4. After separation from the synthesis gas, hydrogen can be used as fuel, while no CO<sub>2</sub> is emitted during combustion.

Oxy-fuel combustion differs from pre-combustion capture as the sequestration approach is based on the oxidizer rather than the fuel being burned, supplying oxygen instead of air to the combustion. The oxygen is typically separated from air by cryogenic distillation in an air separation unit (ASU). A consequence of combustion with oxygen is higher flame temperatures, which can be critical with respect to material constraints. This can be addressed by recirculating part of the flue gas after recovering its sensible heat, thereby reducing the flame temperatures. The flue gas consists mainly of CO<sub>2</sub> and water, which can easily be removed by condensation, leaving behind a relatively pure CO<sub>2</sub> stream [5]. The advantage of this sequestration technique is the simplicity of isolating the CO<sub>2</sub>, while the main disadvantage lies in the high energy demand for purifying oxygen with an ASU. Cryogenic distillation is based on cooling down a stream of compressed air to the point when its components liquify. This allows distillation of the main components, oxygen, nitrogen and argon into relatively pure separate streams [17].

## 2.3 Carbon Utilization

Captured  $\text{CO}_2$  can either be sequestered in a natural sink or utilized as a product or feedstock for other processes. Examples of direct utilization of  $\text{CO}_2$  are its application as protective gas in the food industry and the carbonation of beverages [18].  $\text{CO}_2$  can also be utilized as feedstock for the production of fuels or chemicals, thereby partially replacing fossil fuels or feedstocks. The conversion of  $\text{CO}_2$  to other products often has intermediate chemicals, such as methane, methanol or synthesis gas, which opens a large variety of possible pathways [19][20]. In the context of a steam cracker plant, the synthesis of methanol followed by the methanol-to-olefins (MTO) process is of obvious interest. Methanol can be synthesized by hydrogenation, which has two main reaction pathways [21][22].



## 2.4 Electrified Steam Methane Reforming

Hydrogen is another essential material of the chemical industry, fulfilling various roles along the chemical value chain. Furthermore, hydrogen is considered to likely play an increasingly important role in future energy systems, with potential applications ranging from transportation, residential and industrial heat supply, stationary power generation and energy storage [23].

Currently, hydrogen is produced almost exclusively from fossil fuels, with methane steam reforming (SMR) being the leading production route [10].

In SMR, methane reacts with steam mainly to hydrogen and carbon monoxide (CO) according to Reaction 2.3, forming a synthesis gas. The reversible Water-Gas Shift Reaction (WGS), Reaction 2.4 also occurs partially during SMR, thus forming  $\text{CO}_2$  in small fractions as well [24].



The endothermic reformation Reaction 2.3 is typically performed at temperature ranges of 750–900 °C and pressure levels ranging from ambient to 30 bars in heated tubes in presence of a usually nickel-based catalyst [25]. Methane present in the reformed gas due to incomplete conversion is usually referred to as methane slip. The energy demand for the reformation is conventionally provided by combustion of fuel gas which is a mixture of natural gas and potential off-gases in most cases [24].

The methane conversion  $x_{\text{CH}_4}$  of SMR can be calculated by the methane moleflows of the reactor inlet and outlet and is defined as follows:

$$x_{\text{CH}_4} = \frac{\dot{m}_{\text{CH}_4_{in}} - \dot{m}_{\text{CH}_4_{out}}}{\dot{m}_{\text{CH}_4_{in}}} \quad (2.5)$$

The concentration of hydrogen in the synthesis gas can be further increased downstream of the reformer by the WGS Reaction 2.4, as the syngas stream typically has a high CO content and sufficient water left to form H<sub>2</sub> and CO<sub>2</sub>. The WGS reaction is moderately exothermic, reversible, equilibrium controlled and typically uses a catalyst [25].

To increase conversion and thereby hydrogen yield, WGS is often carried out in two consecutive reactors with intercooling, where the first WGS reactor has higher operating temperatures than the second. This produces a shifted syngas stream, consisting mainly of H<sub>2</sub>, CO<sub>2</sub> and water, while residual amounts of unreformed methane and a small fraction of CO are typically also present [26]. To obtain purified hydrogen, manifold purification techniques are available, ranging from several adsorption mechanisms, over cryogenic distillation, membranes and metal hydride separation [27]. The selection of the right separation technique depends on the desired purity, temperature and pressure of the isolated hydrogen stream. Pressure Swing Adsorption (PSA) is commonly used in industrial applications, delivering a high purity (99.9 %) hydrogen stream [24]. The concept is based on exploiting the varying adsorption behavior of different molecules and the influence of pressure on it. Pressurized synthesis gas is fed to the adsorption bed where all other molecules and compounds except hydrogen are adsorbed. This is followed by desorption at low pressures close to ambient, leaving behind unpressurized, depleted syngas. By parallel usage of several PSAs, the described batch process can be operated continuously [28]. Hydrogen recovery of PSAs is typically in the range of 75-90 %, which translates to 25-10 % of the hydrogen remaining in the depleted syngas. The depleted syngas can be used as fuel for the SMR reactor, providing the thermal energy for reformation through combustion [24].

SMR is a well established and optimized process for hydrogen production. Among the efforts to further increase process efficiency and reduce emissions of SMR, usage of electricity as an alternative heat source has recently gained increasing interest. Emissions can be significantly reduced, as the combustion of fossil fuel makes up 30-40 % of the roughly 9 kg<sub>CO<sub>2</sub></sub>/kg<sub>H<sub>2</sub></sub> emitted by SMR [10]. Furthermore, the electrification of SMR can help overcome the heat transfer limitations of conventional SMRs, which are considered a bottleneck for efficiency improvements of these reformers. The heat transfer limitation is due to low conductivity of the catalyst bed in the reactor and the alloys from which the reactor tubes are made. The low conductivity leads to steep radial temperature gradients in the reactor tube, causing thermal stress which reduces lifetime and mandates long start-up times for industrial sized reformers [29].

The approach of electrified steam methane reforming (e-SMR) has been studied since 1992, when *Spagnolo et al.* conducted experimental studies on the subject [30]. In the following years, different electric heating methods have been investigated, ranging from induction and microwave heating over resistance-based heating to a hybrid method combining concentrated solar and electric heating [29]. In a recent publication *Wismann et al.* verified a resistance-based heating approach experimentally, and extrapolated the results to industrial size and operating conditions with help of a numerical model. The results showed that heat transfer is no limitation factor of the modelled e-SMR reactor, as the catalyst in the reactor tube is heated directly.

## 2. Theory

---

This allows uniform supply of heat and improved reaction control, while the reactor size can be reduced by two orders of magnitude [12]. Although these results appear promising, the concept still needs to be verified on an industrial scale, for which a pilot plant is currently being built [10].

# 3

## Methods

This chapter covers the methodological approach of this work, which centers around investigating the emission reduction potential of integration scenarios of an e-SMR into an ethane cracker through process modeling using the Aspen Plus® software. Figure 3.1 provides an overview of the individual steps to achieve the objectives of this work.

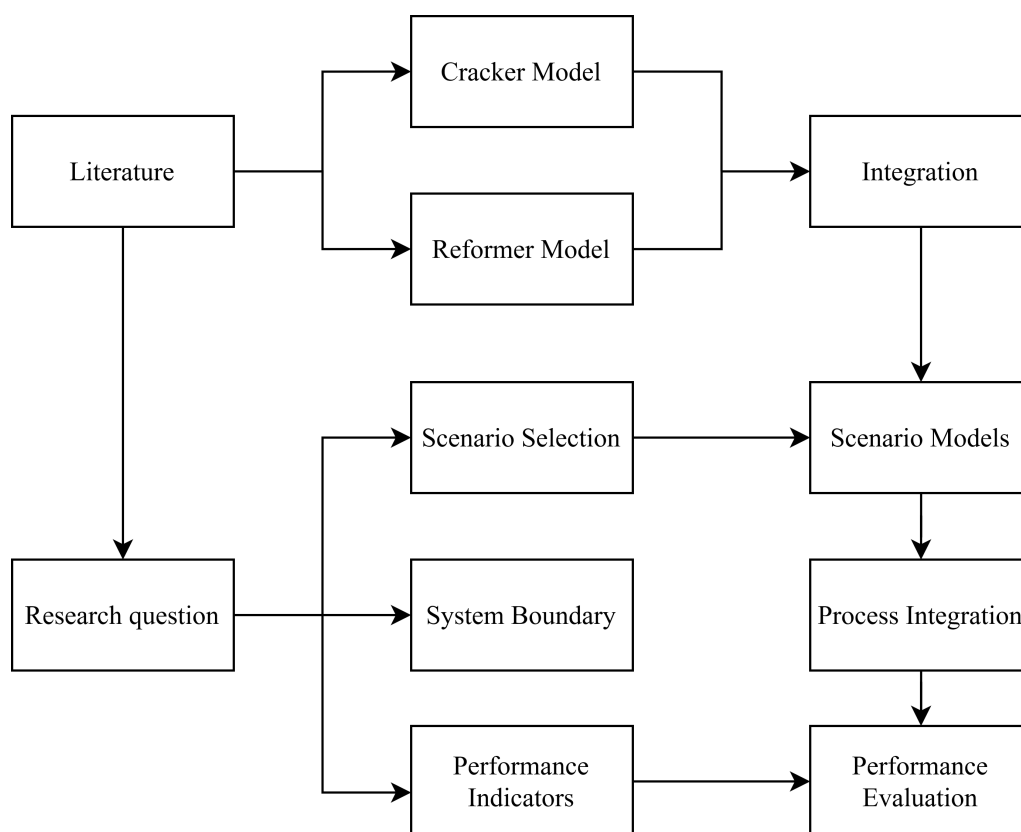


**Figure 3.1:** Methodological approach

Based on a literature review on the investigated processes and auxiliary technology, two stand-alone process simulation models for a cracker furnace and an e-SMR were developed. The system boundary, scenario selection, and key performance indicators (KPIs) for the evaluation were defined with the objective to investigate the emissions reduction potential of integrating e-SMR with an ethane steam cracker. The process models were validated individually with literature data, then the specific scenarios were generated by integrating and modifying the reformer and cracker model. Lastly

data to calculate the performance indicators of the integrated models was extracted to allow discussion of their emission reduction potential.

### 3.1 Scenario Selection

Originating from individual models for a cracker furnace and an e-SMR, two different integration scenarios were selected to investigate their impact on the energy balance of a steam cracker plant and emission reduction potential. One scenario features pre-combustion emission reduction measures, switching and thereby decarbonizing the fuel used in the cracking furnace. The other scenario is based on oxy-fuel combustion, where fuel is burnt with relatively pure oxygen to generate a flue gas stream with high concentration of  $\text{CO}_2$ .

The first scenario is referred to as *Hydrogen Firing* in the following text, because hydrogen replaces the conventional fuel gas, ideally resulting in a  $\text{CO}_2$ -free flue gas stream. A lesser fraction of the hydrogen is obtained directly from the cracked gas, while the larger fraction is converted from methane in the e-SMR. Since e-SMR uses electricity to supply heat to the reforming reaction, this is an example of indirect electrification of a cracker furnace.

The other scenario, referred to as *Oxyfuel*, takes a decisively different approach to isolate carbon emissions. The oxygen required for combustion of the fuel gas is supplied to the furnace in the form of pure oxygen instead of air, hence the name of the combustion regime. This produces a flue gas stream that contains mainly water and carbon dioxide and therefore allows easy separation of the  $\text{CO}_2$ .

### 3.2 System Boundary

The elementary system boundary used in this work can be seen in Figure 3.2, where it is applied to a conventional cracker furnace.

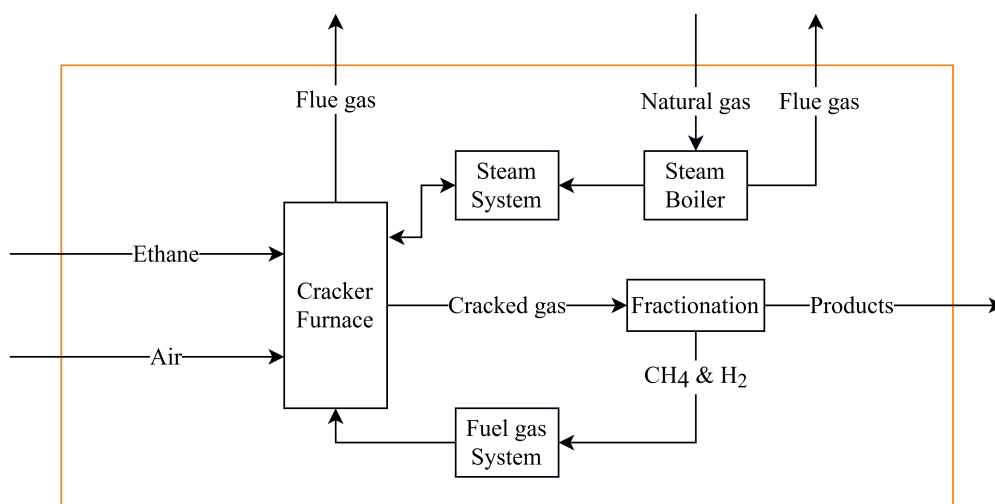


**Figure 3.2:** System Boundary of a conventional cracker furnace

The material stream inputs into this system are the ethane feedstock for cracking and air for combustion in the cracking furnace. Electricity, which is used by a pump to raise the pressure of water before it enters the convection section, is another input not shown in the system boundary. The process streams leaving the system are flue gas originating from combustion and a product stream, containing all cracked gases except the  $\text{CH}_4$  and  $\text{H}_2$ . The multitude of process steps to purify and separate the different compounds in the cracked gas is not considered in detail in this work. The fractionation system displayed in Figure 3.2 is a simplification, representing the isolation of the light hydrocarbons  $\text{CH}_4$  and  $\text{H}_2$  in the demethanizer [31]. Further simplifications apply to the steam and flue gas systems, which both are considered net balances. This means they are both able to supply and accommodate required mass flows, while the net mass flow of all inputs and outputs is taken into account in the further work. The steam generated by heat recovery in the convection part and in the TLE of the cracker furnace is fed into the steam system, while the dilution steam is considered as consumption. In case of a steam deficit a natural gas boiler generates additional steam using methane as fuel. The fuel gas system is needed to supply additional fuel gas to the furnace, since ethane crackers are typically not self-sufficient when burning solely the fuel grade byproducts contained in the cracked gas. The output of this system is assumed to be a stable and homogeneous mixture of 50/50 mol%  $\text{CH}_4$  and  $\text{H}_2$ . In a cracker plant with different cracker furnace types, the fuel gas system would be fed by several streams of  $\text{CH}_4$  and  $\text{H}_2$  coming from different furnaces.

Integrating an e-SMR into this system has implications on the process streams, resulting in an adopted system boundary for each scenario. Figure 3.3 depicts the system boundary for *Hydrogen Firing*.

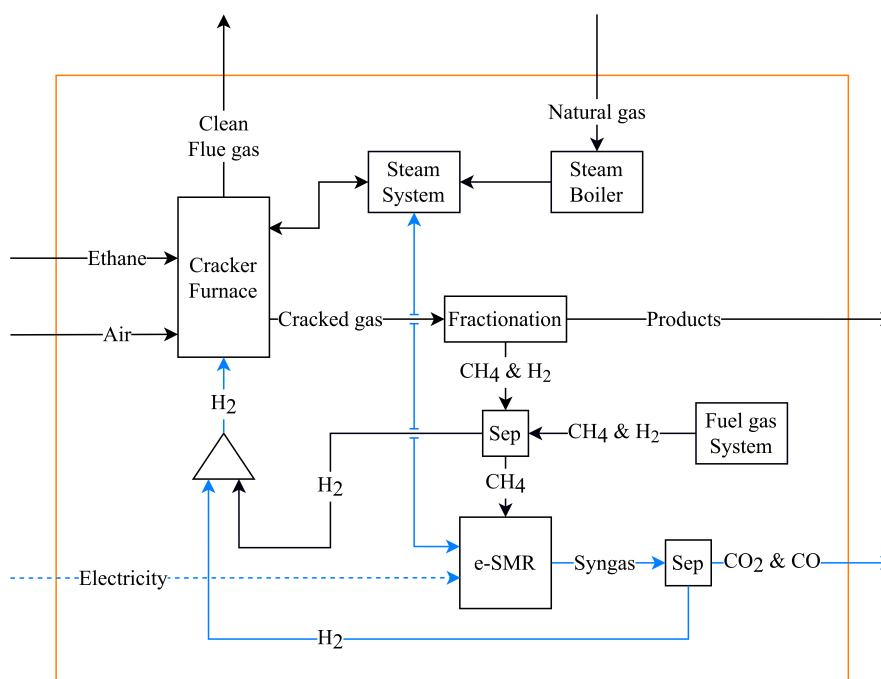


**Figure 3.3:** System Boundary for the *Hydrogen Firing* scenario

The process streams that were modified to integrate the e-SMR are highlighted in blue. A new input stream to the system is the electricity that is supplied to the e-SMR. The  $\text{CH}_4$  and  $\text{H}_2$  contained in the cracked gas are not sent to the fuel gas system but used as feedstock for reformation. Hydrogen is separated and bypasses the reformer, to allow maximum methane conversion in the e-SMR. The reformation of methane produces synthesis gas which is shifted via WGS to increase hydrogen yield. The hydrogen is separated from the shifted syngas and mixed with the by-passed hydrogen stream. This stream of hydrogen is combusted in the cracker furnace, but does not provide sufficient energy for cracking. Therefore additional fuel gas is drawn from the fuel gas system and also flows through the described sequence of separation and reformation. The separation of hydrogen from the reformed syngas leaves a stream of depleted synthesis gas behind, which consists largely of  $\text{CO}_2$ ,  $\text{H}_2$  and  $\text{CH}_4$  and is the only additional output of the modified system boundary.

Integrating the e-SMR into a steam cracker powered by oxy-fuel combustion results in the system boundary presented in Figure 3.4, in which the modified process streams are highlighted.

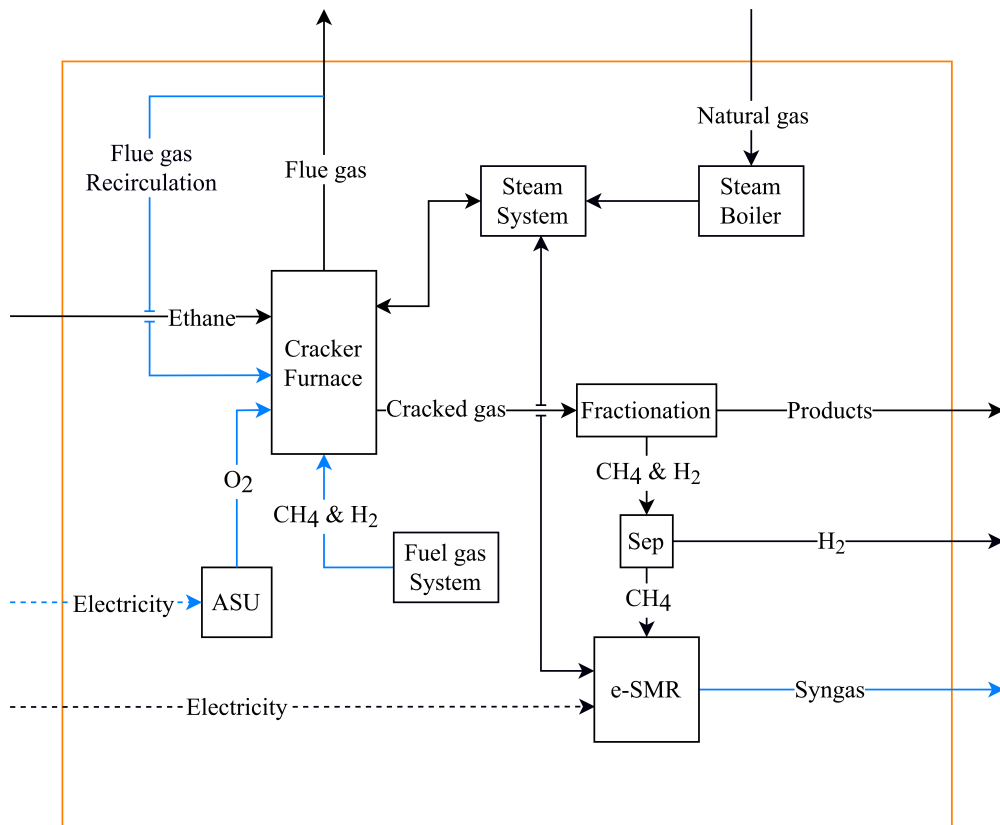


**Figure 3.4:** System Boundary for the *Oxyfuel* scenario

As described in Chapter 2.2, oxy-fuel combustion is based on burning fuel gas with a stream of relatively pure oxygen instead of air. This work assumes the utilization of an ASU to supply oxygen. This adds a new component, which is the second significant electricity consumer besides the e-SMR, to the system boundary. Another

characteristic of oxy-fuel combustion is the recirculation of flue gas to decrease the flame temperatures. The fuel gas is drawn exclusively from the fuel gas system in this scenario. Hydrogen separated from the cracked gas is leaving the system boundary, as well as shifted synthesis gas reformed in the e-SMR.

### 3.3 Performance Indicators

Several Key Performance Indicators (KPIs) are used to evaluate the impact of the integration scenarios on the energy balance and emissions of the steam cracker model. Table 3.1 provides an overview of the KPIs selected for this work, whose definitions are explained in the following. All mass and energy flows are normalized to the main product of the considered ethane cracking process, ethylene.

The system efficiency  $\eta$  is used to evaluate energetic performance of each scenario according to its system boundary and is defined as follows:

$$\eta = \frac{\sum E_{out}}{\sum E_{in}} \quad (3.1)$$

All energy flows according to the system boundary are considered for the system efficiency. For the material streams that are combustible, the higher heating value is used to estimate their energy content. The energy associated with the net steam generation is calculated based on the enthalpy difference between the pressurized steam and atmospheric boiler feedwater at 10 °C.

The specific energy consumption (SEC) describes how much energy is consumed within the considered system boundary for producing a unit of ethylene and is calculated as shown in Equation 3.2. Energy consumption is composed of combustion heat and electricity consumption.

$$SEC = \frac{Q_{Comb} + W_{Elec}}{\dot{m}_{Ethylene}} \quad (3.2)$$

The net steam generation (NSG) is essentially the internal balance of the steam system. Positive contribution to the balance are steam generation by heat recovery within both the cracker and reformer model. Each of these models also has an internal steam consumption, which is a negative contribution to the balance. In the cracker, steam is needed to dilute the feedstock, while the reformer needs steam as a reactant. It is assumed that the net steam generation of the base case must be maintained. In cracker plants, steam is often used to drive compressors and refrigeration cycles in the fractionation system. If the net steam generation of a scenario is smaller than the base case, the deficit will be compensated by the natural gas boiler, which will affect the SEC and emissions of the system. A larger net steam generation on the other hand will not impact any other KPIs than the NSG; theoretically, the steam could be used to generate electricity in a turbine. To estimate the steam generation potential of heat integration of the coolers in the reformer, a pinch analyses was conducted, which can be found in Appendix A. The

### 3. Methods

---

calculations for the energy consumption and emissions associated with the steam boiler are presented in Appendix B.

$$NSG = \frac{\dot{m}_{SteamProd} - \dot{m}_{SteamCon}}{\dot{m}_{Ethylene}} \quad (3.3)$$

The specific fuel gas consumption (SFG) simply accounts for the fuel gas drawn from the fuel gas system.

$$SFG = \frac{\dot{m}_{FuelGas}}{\dot{m}_{Ethylene}} \quad (3.4)$$

For specific emissions (SE), only CO<sub>2</sub> is considered. Other compounds containing carbon are converted to CO<sub>2</sub> on molar bases, as if they were fully oxidized. Specific emissions can be composed of various hydrocarbon streams, primarily emissions from fuel combustion, but also synthesis gas streams and emissions associated with electricity. To quantify emissions associated with electricity consumption, a carbon intensity of 55 g<sub>CO<sub>2</sub></sub>/kWh for the Swedish grid was assumed [32].

$$SE = \frac{\dot{m}_{CO_2}}{\dot{m}_{Ethylene}} \quad (3.5)$$

**Table 3.1:** Overview of the KPIs

KPI	Unit	Abbreviation
System Efficiency	%	-
Specific Energy Consumption	MJ/kg <sub>Ethylene</sub>	SEC
Net Specific Steam Generation	kg <sub>Steam</sub> /kg <sub>Ethylene</sub>	NSG
Specific Fuel Gas Consumption	kg <sub>Fuelgas</sub> /kg <sub>Ethylene</sub>	SFG
Specific Emissions	kg <sub>CO<sub>2</sub></sub> /kg <sub>Ethylene</sub>	SE

# 4

## Process Modeling

This chapter summarizes the assumptions made and modeling tools used in this work. The process parameters and control system of the conventional cracker and reformer model are presented, followed by a description of the modifications required to create the two integration scenarios.

The simulation tool used to develop process models of the analyzed system is *Aspen Plus® V12.1*. The property method GRAYSON was selected for calculating thermodynamic properties of components. Different types of manipulators are available to allow the user to define process parameters. This chapter will only briefly describe the function of the manipulators to show the operating principles of the models, while the detailed specifications can be found in Appendix C.

Model assumptions:

- steady state operation
- constant gas composition for feedstock, fuel gas and reactor yields
- no pressure drop over heat exchangers and reactors
- no thermal resistance within heat exchangers
- no char formation

### 4.1 Cracker Furnace

The process model of the cracker furnace is reduced to the most significant parts needed for this work, which is the radiation and convection section of the furnace as well as the TLE.

#### 4.1.1 Model Description

The radiant section is modeled as two linked reactors, one representing the combustion of fuel gas by burners and the other representing the tubular reactor in which the feedstock is cracked.

A *RGibbs* reactor was selected to estimate the heat generated by the combustion of fuel gas. This reactor block is based on the minimization of total Gibbs free energy to calculate the equilibrium compositions of any reacting system. By specifying the mass flow and composition of the feed stream, the possible products, as well as reactor pressure and outlet temperature, the reactor calculates the heat duty according to these inputs.

The cracking of ethane was modeled using a *RYield* reactor that allows the com-

position of the output stream to be specified in addition to the general process parameters feed mass flow and composition, reactor pressure and temperature. By defining the outlet gas composition, the reactor calculates the heat demand according to the process parameters.

The convection section of the furnace was modelled with several multi-stream-heat exchangers (*MHeatX*). These heat exchangers are used to represent the heat recovery measures applied in a conventional cracker furnace. During quenching of the cracked gas in the TLE, water is heated and evaporated, which is modeled with two heat exchangers. The thermal energy of the hot flue gases is recovered by preheating water and feedstock, while also superheating the steam coming from the TLE. Figure 4.1 illustrates the layout of the heat exchangers, while Table 4.1 presents the constraints specified in the model.

The process parameters and gas compositions for the cracker model are summarised in Table 4.2

**Figure 4.1:** Convection section of the modeled cracker furnace

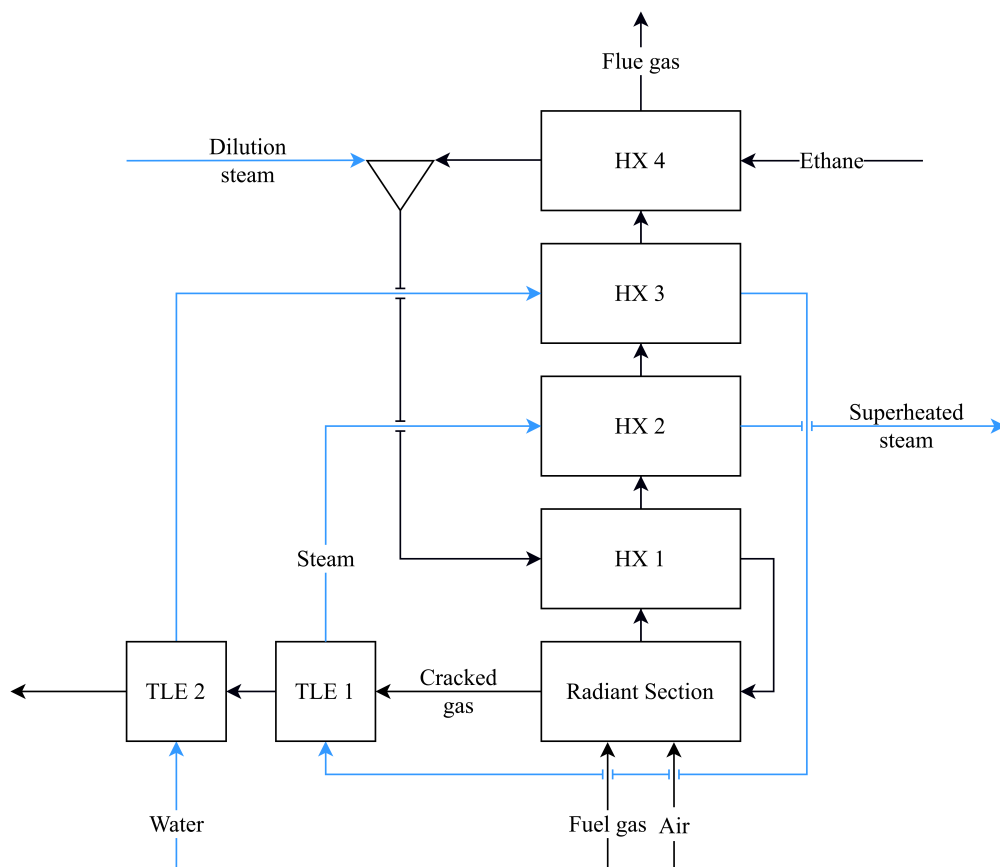


**Table 4.1:** Specified constraints for heat integration

	<b>Constraint</b>	<b>Value</b>
HX 1	Cold outlet temperature	650 °C
HX 2	Cold outlet temperature	450 °C
HX 3	Cold outlet vapour fraction	0
HX 4	Hot outlet temperature	160 °C
TLE 1	Cold outlet vapour fraction	1
TLE 2	Hot outlet temperature	200 °C

**Table 4.2:** Parameters of the cracker model

<b>Process conditions</b>	<b>Parameter</b>	<b>Unit</b>
Cracking reactor		
Reactor inlet temperature	650	°C
Reactor outlet temperature	840	°C
Reactor pressure	3.2	bar
Feed	Ethane	
Dilution steam temperature	240	°C
Dilution steam pressure	8.8	bar
Feed to steam ratio	3	
Combustion reactor		
Reactor inlet temperature	650	°C
Reactor outlet temperature	1200	°C
Fuel grade cracked gas	8 mol% $CH_4$ , 92 mol% $H_2$	
Fuel gas	50 mol% $CH_4$ , 50 mol% $H_2$	
Oxygen to fuel ratio	1.05	
Combustion efficiency	95	%
Oxy-fuel combustion		
Flue gas recirculation	80	%
ASU		
Oxygen output	95 mol% $O_2$ , 5 mol% $Ar$	
Electricity consumption	0.294	kWh/kg

### 4.1.2 Control System

This section briefly describes the function of the main manipulators used to control the model.

The two reactors representing the combustion of fuel gas and cracking of ethane are coupled through their heat demand/surplus by a *Design Specification*. These manipulators allow the user to define a target value for a process parameter and specify another parameter that will be varied to reach that target value. In this manner the mass flow of fuel gas fed to the combustion reactor is adjusted to match its heating duty with the energy demand of the cracking reactor, which is determined by its inputs.

Another *Design Specification* is implemented to estimate the mass flow of the steam generation in the cracker. The mass flow of water is varied to obtain the specified flue gas temperature, see HX 4 in Table 4.1, before the flue gas exits the convection section of the cracker furnace.

A simple *Calculator* is used to calculate and set the mass flow of air entering the combustion reactor to the desired oxygen to fuel ratio. The mass flow of the dilution steam is set in similar manner according to the feed of ethane entering the yield reactor. For the *Oxyfuel* scenario, the electricity consumption of the ASU is implemented with a *Calculator*.

### 4.1.3 Validation

The presented model of a steam cracker furnace was validated against available literature values which are scarce and often differ in definitions. For this purpose, the fuel gas was changed to pure methane, as this is the case in the literature used [4]. The KPIs for the modified model, as well as the conventional model and literature values are shown in Table 4.3.

**Table 4.3:** KPIs of the conventional cracker model, modified cracker model and literature values

KPI	Model used	Model modified for validation	Literature values	Unit
SEC	16.9	17.5	9-19	MJ/kg <sub>Ethylene</sub>
SNSG	2.2	3		kg <sub>Steam</sub> /kg <sub>Ethylene</sub>
SFGC	0.3	0.53		kg <sub>Fuelgas</sub> /kg <sub>Ethylene</sub>
SE	0.71	0.96	1.0-1.2	kg <sub>CO<sub>2</sub></sub> /kg <sub>Ethylene</sub>

The SE of 0.96 kg<sub>CO<sub>2</sub></sub>/kg<sub>Ethylene</sub> is slightly lower than the literature values reported as 1.0-1.2 [4]. To compare the SEC the reported literature value had to be converted, as its definition includes energy used for separation. The converted values range from 9-19 MJ/kg<sub>Ethylene</sub>, thereby only representing energy inputs into the cracker furnace as defined in this work. The SEC of the modified cracker model used for validation has a value of 17.5 which is within the derived range but at its upper end. The increase of the NSG from 2.2 to 3 when modifying the cracker model for validation stems from differing mass flows and composition of the flue gas, as the fuel gas was changed from a mixture of 50/50 mol% CH<sub>4</sub> and H<sub>2</sub> to pure CH<sub>4</sub>. Hydrogen in the fuel gas reduces CO<sub>2</sub> concentration of the flue gas, while increasing its H<sub>2</sub>O concentration. As the two compounds have different heat capacities, the sensible heat of the flue gas streams differs as well, which is used to generate steam in the TLE and convection section of the cracker. The reduction of SE by burning a 50/50 mol% mix of methane and hydrogen shows how adding hydrogen to the fuel gas is an effective emissions reduction measure.

## 4.2 Reformer

### 4.2.1 Model Description

Figure 4.2 gives an overview of the process model representing an e-SMR.

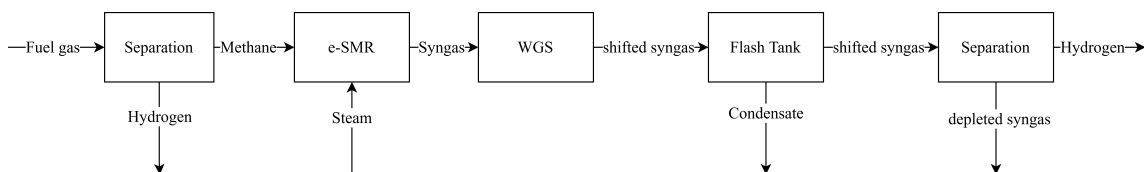


**Figure 4.2:** Flowsheet of the reformer model

The input to the reformer model is the  $\text{CH}_4$  and  $\text{H}_2$  separated from the cracked gas, which is compressed to reach the operating pressure of the e-SMR. The hydrogen is separated from the methane to bypass the reformer before steam is added to the methane and the mixture is preheated and then fed to the reformer. To estimate the electricity consumption of an e-SMR a *RGibbs* reactor was chosen, as it allows the specification of an approach temperature, which restricts the chemical equilibrium. With the possible products, the feed composition and reactor pressure and inlet temperature defined, the reactor block outputs the heat demand needed to reach chemical equilibrium. It is assumed that this heat will be supplied by resistance heating without losses. The hot syngas leaving the reactor is cooled by heat exchange against the feed. Shifting of the syngas to increase hydrogen yield is conducted in two WGS reactors with intercooling. Adiabatic *REquil* reactors are chosen to represent the WGS reactors. Downstream of the WGS reactors the residual water in the syngas is condensed in a flash tank. After the final separation of hydrogen from the shifted syngas, a stream of depleted syngas consisting mainly of  $\text{CO}_2$  and methane is left behind. The reformed hydrogen is mixed with the bypassed hydrogen stream. For the separation of hydrogen from other gases a hybrid system consisting of a membrane and a PSA is assumed. The hydrogen is pre-enriched through the membrane and then fed into the PSA to achieve a high degree of purity. The system works at elevated pressure, while the offgas leaves the PSA depressurized [33]. This separation system was implemented as one separation block in the process model, with specifications according to literature which are presented in Table 4.4.

**Table 4.4:** Parameters of the e-SMR model

Process conditions	Parameter	Unit
e-SMR		
Reactor inlet temperature	466	°C
Reactor outlet temperature	920	°C
Temperature approach to equilibrium	20	°C
Reactor pressure	27.7	bar
Feed	66 mol% $CH_4$ , 34 mol% $H_2$	
Dilution steam temperature	411	°C
Dilution steam pressure	27.7	bar
Steam to carbon ratio	1.8	
High Temp. WGS Reactor		
Reactor inlet temperature	350	°C
Low Temp. WGS Reactor		
Reactor inlet temperature	150	°C
PSA Membrane System		
Hydrogen purity	100	%
Hydrogen selectivity	90	%
Exhaust gas pressure	1	bar

### 4.2.2 Validation

The e-SMR model was validated against a recent publication about the electrification of SMR, which uses a combined approach of experiments and numerical modelling [12]. The study investigated a lab-scale e-SMR reactor operated at ambient pressure and applied the measured results to a numerical model. Subsequently the numerical model was extrapolated to industrial conditions.

The reactor parameters are specified in the publication, as well as the resulting methane conversion  $x$ , but no gas composition is presented. Table 4.5 shows the conversion reported in the publication and conversion achieved by the model used in this work operated at the same process parameters.

**Table 4.5:** Validation e-SMR

	Model	Literature	Deviation
Methane conversion	74.2 %	75.4 %	1.3 %

The deviation between the methane conversion of the model and the value reported in the literature is in an acceptable range, therefore it is assumed from here on, that the reactor model of an e-SMR can be used for this work.

# 5

## Results and Discussion

This chapter presents the KPIs obtained from the two integration scenarios and addresses their impact on an ethane cracker. First the scenarios are discussed individually before comparing their emission reduction potential.

### 5.1 Hydrogen Firing

The *Hydrogen Firing* scenario aims to reduce cracker furnace emissions by switching the fuel to hydrogen. A lesser fraction of the hydrogen needed for sufficient heat supply is already present in the cracked gas stream, while the larger fraction is produced by reformation of  $\text{CH}_4$  in an e-SMR. Ethane crackers are not self-sufficient when all the fuel-grade by-products are burnt directly, therefore it is no surprise that this is also the case when  $\text{H}_2$  reformed from  $\text{CH}_4$  is combusted. To supply sufficient heat to the cracker additional fuel gas from the fuel gas system is therefore fed to the reformer. Separating the hydrogen from the syngas to combust it in the cracker furnace leaves behind a stream of depleted syngas, which contains the carbon. Table 5.1 presents the KPIs generated by the process model of this integration scenario.

**Table 5.1:** KPIs *Hydrogen Firing*

KPI	Value	Unit
System efficiency	88.6	%
SEC	18	MJ/kg $_{Ethylene}$
NSG	1.9	kg $_{Steam}$ /kg $_{Ethylene}$
SFG	0.09	kg $_{Fuelgas}$ /kg $_{Ethylene}$
Indirect Emissions	0.041	kg $_{CO_2}$ /kg $_{Ethylene}$
SE	0.4	kg $_{CO_2}$ /kg $_{Ethylene}$

The system efficiency decreases by 7.4 % compared to the model of a conventional steam cracker. The main reason for this is the additional energy input in form of electricity to power the e-SMR. Since this electricity is used to generate pure hydrogen from an already combustible gas mix, the energy input to the system increases significantly which reduces the system efficiency. The power demand of the e-SMR also increases the SEC of this scenario compared to a conventional cracker. In addition, the specific steam production decreases with respect to a conventional cracker. This can be attributed to the decrease of sensible heat contained in the flue gas stream, which is used to superheat and preheat steam and feedstock in the convection section of the cracker furnace. The reason for this is primarily the

decreased flue gas mass flow and the fact that no  $\text{CO}_2$  is present in the flue gas stream. Based on the assumption that the net steam generation of the conventional must be maintained, the steam deficit is compensated by combusting natural gas in the steam boiler to generate steam. The SFG significantly decreases as the fuel grade component of the cracked gases is used as fuel after reformation, which is not the case in the conventional cracker model. The specific indirect emissions associated with electricity contribute with approximately 10 % to the total specific emissions. The other 90 % stem from the depleted syngas generated by separation of hydrogen after reformation. The depleted syngas leaving the system boundary consists mainly of  $\text{CO}_2$ ,  $\text{H}_2$  and  $\text{CH}_4$ . Hydrogen is present in the depleted syngas due to the imperfect separation of hydrogen with the hybrid PSA-membrane system. A detailed composition is shown in Table 5.2.

**Table 5.2:** Depleted syngas composition *Hydrogen Firing*

Component	mol-%
$\text{CO}_2$	50.7
$\text{H}_2$	24.8
$\text{CH}_4$	22.3
CO	1.9
$\text{H}_2\text{O}$	0.3

## 5.2 Oxyfuel

The *Oxyfuel* scenario aims to reduce cracker emissions by concentrating them in the flue gas stream. This is achieved by combusting fuel gas with relatively pure (95 %) oxygen generated by an ASU. The  $\text{CH}_4$  present in the cracked gases is reformed to syngas rich in hydrogen and can be further processed or sold.

The KPIs of the process model for the *Oxyfuel* scenario are presented in Table 5.3.

**Table 5.3:** KPIs *Oxyfuel*

KPI	Value	Unit
System efficiency	93.8	%
SEC	18.6	$\text{MJ}/\text{kg}_{\text{Ethylene}}$
NSG	2.2	$\text{kg}_{\text{Steam}}/\text{kg}_{\text{Ethylene}}$
SFG	0.28	$\text{kg}_{\text{Fuelgas}}/\text{kg}_{\text{Ethylene}}$
Indirect Emissions	0.038	$\text{kg}_{\text{CO}_2}/\text{kg}_{\text{Ethylene}}$
SE	0.86	$\text{kg}_{\text{CO}_2}/\text{kg}_{\text{Ethylene}}$

The system efficiency of the *Oxyfuel* scenario is higher than for *Hydrogen Firing*, while it decreases by 2.2 % compared to the model of a conventional cracker. The reason is presumably the smaller electricity consumption of the e-SMR, as less  $\text{CH}_4$  is reformed. While the ASU is an additional consumer, the total electricity usage is smaller for *Oxyfuel* compared to *Hydrogen Firing*.

The SEC of *Oxyfuel* is higher than both the conventional cracker and *Hydrogen Firing* models. This is due to the fact that similar amounts of fuel gas are burnt as

in the conventional cracker model, while energy for reformation and air separation is also consumed.

NSG is approximately equal to a conventional cracker and can therefore satisfy the energy demand for refrigeration and compression in the fractionation. The reason for this can again be found in the mass flow and composition of the flue gases. Since no nitrogen is present during combustion the mass flow is smaller. This seems to be compensated by increased amounts of CO<sub>2</sub> and the recirculation of flue gas.

The fuel gas consumption of the *Oxyfuel* scenario is slightly lower than for the conventional cracker. Since the same heat demand has to be supplied to the cracking reaction, the difference must stem from the fact that no nitrogen is present in the oxidizer which would be heated during combustion.

Specific emissions of the *Oxyfuel* scenario are higher than for the conventional cracker model. The main fraction of the emissions is present highly concentrated in the flue gas, while a smaller fraction is present in the shifted syngas. Tables 5.4 and 5.5 show the composition of both streams.

**Table 5.4:** Shifted syngas composition *Oxyfuel*

Component	mol%
H <sub>2</sub>	78.9
CO <sub>2</sub>	13.3
CH <sub>4</sub>	7.2
CO	0.6

**Table 5.5:** Flue gas composition *Oxyfuel*

Component	mol%
CO <sub>2</sub>	83.1
Ar	11.1
O <sub>2</sub>	3.6
H <sub>2</sub> O	2.2

If hydrogen were to be used or sold as a pure product stream, separation of it from the shifted gas stream would leave behind depleted syngas of similar composition as presented in Table 5.2. Using this stream of depleted syngas as additional fuel for combustion would serve the purpose of concentrating emissions of *Oxyfuel* in one stream. Another scenario in which depleted syngas from the reformer is fed to the cracker is therefore added. This scenario will be named *Oxyfuel V2*, while the initial *Oxyfuel* scenario will be referred to as *Oxyfuel V1* from hereon. The modified system boundary for *Oxyfuel V2* can be found in Appendix D, while its KPIs are presented in Table 5.6.

**Table 5.6:** KPIs *Oxyfuel V2*

KPI	Value	Unit
System efficiency	93.2	%
SEC	19.4	MJ/kg <sub>Ethylene</sub>
NSG	2.4	kg <sub>Steam</sub> /kg <sub>Ethylene</sub>
SFG	0.27	kg <sub>Fuelgas</sub> /kg <sub>Ethylene</sub>
Indirect Emissions	0.039	kg <sub>CO<sub>2</sub></sub> /kg <sub>Ethylene</sub>
SE	0.84	kg <sub>CO<sub>2</sub></sub> /kg <sub>Ethylene</sub>

Adding the depleted syngas to the cracker furnace decreases system efficiency, while it increases SEC. The reason for this lays in the combustion of unreformed CH<sub>4</sub>

and residual  $H_2$  in the depleted syngas, left behind from separating  $H_2$  from the shifted syngas. It can be seen that this slightly decreases the fuel gas consumption of *Oxyfuel V2*, but it also leads to increased demand of oxygen and therefore higher electricity consumption. The increase in electricity consumption seems to outweigh fuel gas savings, therefore increasing SEC of *Oxyfuel V2*. The flue gas stream is enlarged when re-feeding depleted syngas to the combustion, which increases the NSG. Caused by the reduction of fuel gas, the SE of *Oxyfuel V2* are slightly lower than *Oxyfuel V1*. The increase in indirect emissions associated with electricity consumption from *Oxyfuel V1* to *Oxyfuel V2* is insignificant for this.

### 5.3 Comparison of the Scenarios

After presenting the KPIs of the individual scenarios and elaborating the reasoning behind differences between them, the following section will discuss the main differences between the scenarios and their emissions reduction potential with the help of Figures plotting the KPIs against each other.

Figure 5.1 juxtaposes SEC and NSG of the three scenarios presented.

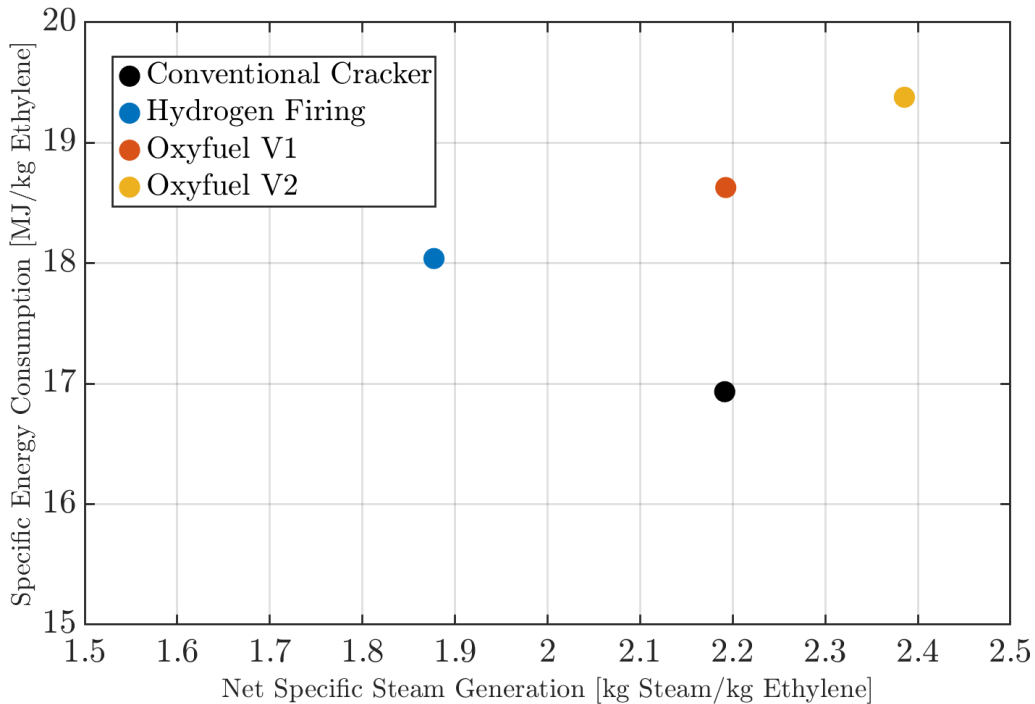


**Figure 5.1:** Specific energy consumption and net steam generation of the investigated scenarios

The figure shows that the carbon mitigation measure of integrating an e-SMR increases the specific energy consumption of the cracker furnace in all scenarios. The impact on the net steam generation varies. *Hydrogen Firing* has the lowest increase in energy consumption, but also greatest decrease in net steam generation. To compensate for this deficit, steam is generated by the steam boiler, but the associated energy and steam generation is not accounted for in this figure. *Oxyfuel V1* has

approximately the same net steam generation as the conventional cracker, but increases the SEC more than *Hydrogen Firing*. *Oxyfuel V2* has the highest SEC, but also generates more steam than a conventional cracker.

While steam is an essential utility for a cracker plant, the focus of this work lies on the emission reduction potential and the associated energy penalty. Figure 5.2 therefore presents the relation between the additional specific energy consumption and the uncaptured emissions for the analysed scenarios.

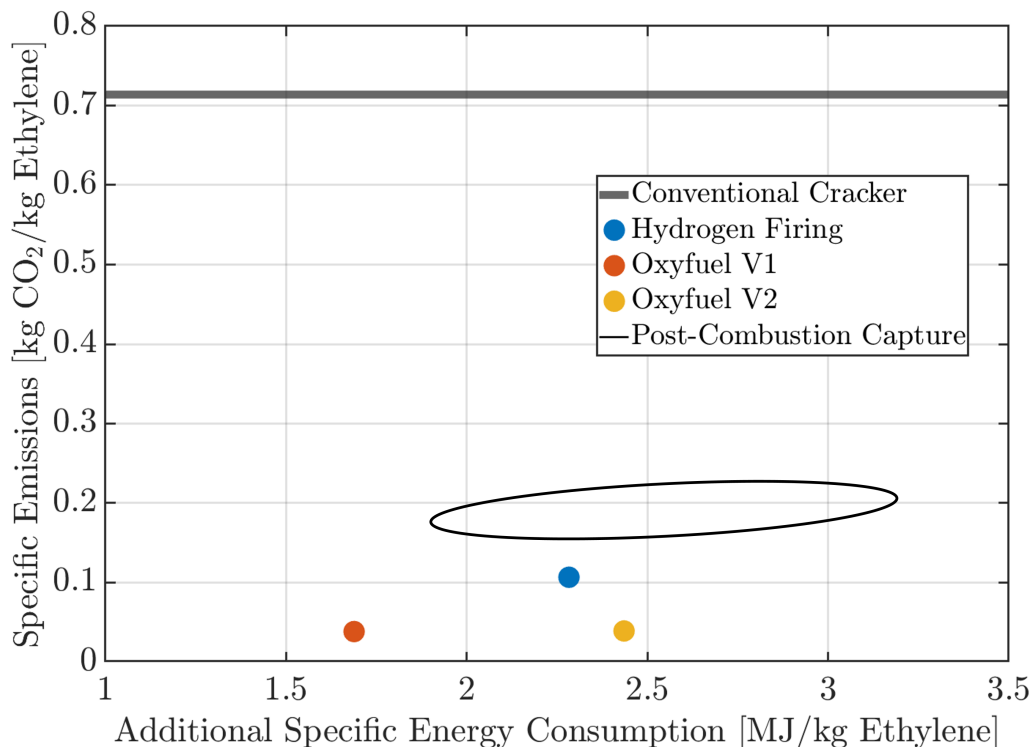


**Figure 5.2:** Specific uncaptured emissions associated with the investigated scenarios compared to a conventional cracker (solid line) and a conventional cracker with post-combustion CO<sub>2</sub> capture (ellipse), plotted against the additional specific energy consumption required for emission reduction

The baseline specific emissions of the conventional steam cracker model are represented by the grey line at 0.7 kg<sub>CO<sub>2</sub></sub>/kg<sub>Ethylene</sub>. Depending on the fuel gas composition this value could increase to 0.96 kg<sub>CO<sub>2</sub></sub>/kg<sub>Ethylene</sub> if pure CH<sub>4</sub> is burned, as Table 4.3 showed. Furthermore, the KPIs of retrofitting a post combustion carbon capture plant to the conventional cracker model have been estimated to showcase the performance of the modelled scenarios against this available emission reduction measure. The black ellipse represents amine-based post-combustion CO<sub>2</sub> capture with an assumed energy demand for regeneration of the solvent ranging from 3-5 MJ/kg<sub>CO<sub>2</sub></sub>, using MEA as absorbent with a 90% CO<sub>2</sub> capture rate.

The emissions on y-axis are considered uncapturable and stem mostly from the indirect emissions associated with the electricity consumed in the modeled scenarios. In the *Hydrogen Firing* scenario, additional emissions are also generated by the steam boiler, which compensates for the steam production deficit.

Both *Oxyfuel* scenarios achieve the largest emission reduction but vary in their additional energy consumption. Feeding depleted syngas from the reformer to the combustion increases the energy consumption, as discussed in detail earlier. *Hydrogen Firing* consumes slightly less energy per kg ethylene, than *Oxyfuel V2*, but leaves more emissions behind. The estimated energy consumption for post-combustion CO<sub>2</sub> capture ranges from 1.9-3.2 MJ/kg<sub>Ethylene</sub> but leaves behind significantly more emissions uncaptured.

Figure 5.2 shows that emission reduction is significant for all scenarios when compared to a conventional ethane cracker. The *Oxyfuel* scenarios achieve the highest reduction of emissions, leaving behind only 5-6 % of the emissions of the conventional cracker model. *Hydrogen Firing* achieves an emissions reduction of 85 % in this framework. However, a significant portion of the uncaptured emissions in this scenario come from the steam boiler. The assumption that the net steam generation of a conventional cracker has to be upheld has a significant impact on the KPIs. Figure 5.3 shows the emission reduction potential of the scenarios if this assumption is neglected. This is especially interesting in the context of electrifying the compressors of the fractionation section.

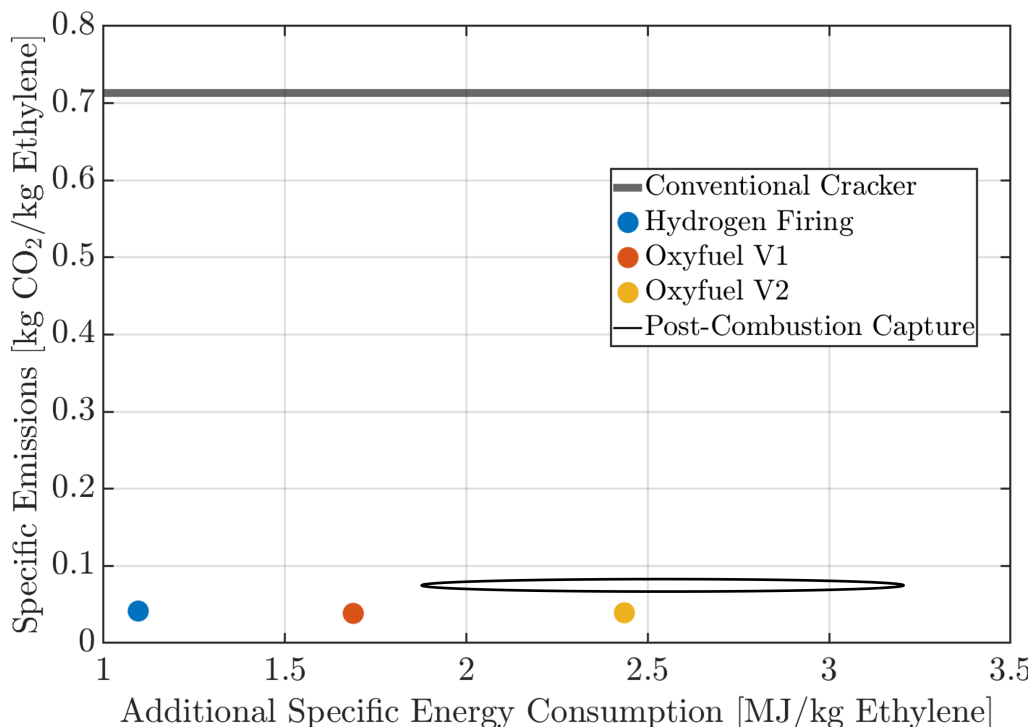


**Figure 5.3:** Specific uncaptured emissions associated with the investigated scenarios compared to a conventional cracker (solid line) and a conventional cracker with post-combustion CO<sub>2</sub> capture (ellipse), plotted against the additional specific energy consumption required for emission reduction, excluding steam generation by a steam boiler

Neglecting the assumption that the net steam generation of the conventional cracker model must be upheld, impacts the KPIs of the *Hydrogen Firing* case as well as the estimate of post combustion carbon capture with amines, as both of them have a

steam deficit. If only indirect emissions are left uncaptured, the reduction potential of all three modeled scenarios is approximately 95 % reduction of the conventional cracker model's emissions to the atmosphere. For conventional post-combustion capture, the uncaptured emissions decrease according to the carbon capture efficiency assumed. Furthermore, the additional energy consumption of *Hydrogen Firing* dropped significantly. After analyzing the energy penalty for emission reduction in the modeled scenarios, the question arises in what form the carbon of the abated emissions is present. Figure 5.4 gives an overview of the different carbon streams of each scenario.

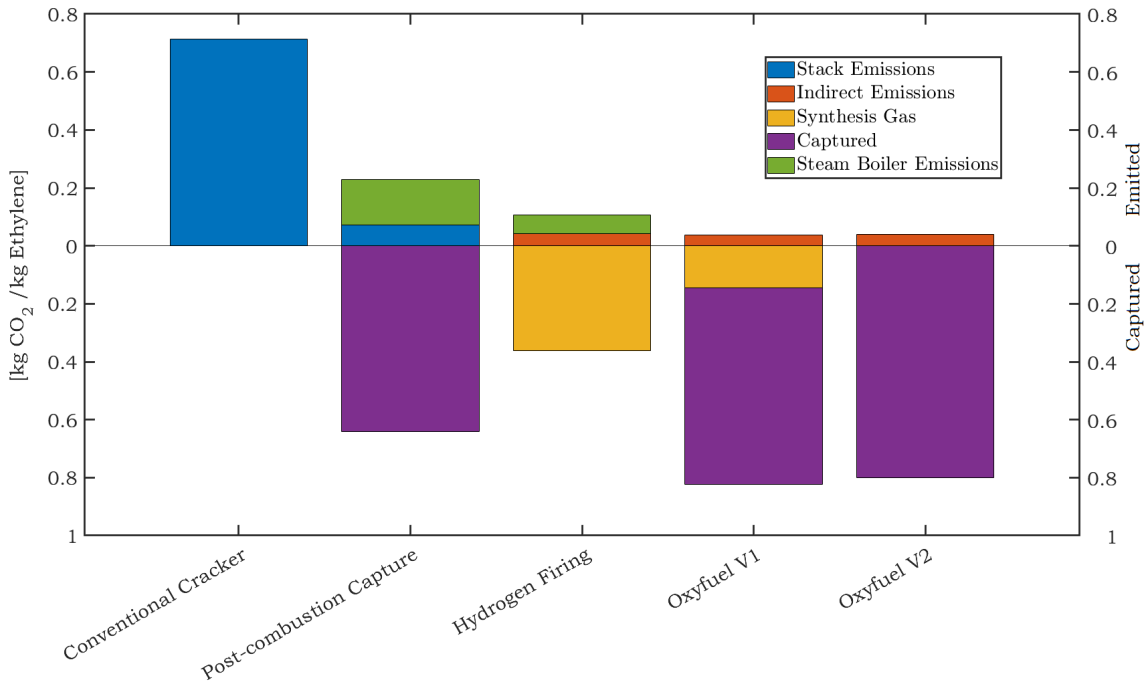


**Figure 5.4:** Emission composition of the investigated scenarios

The upper half of the y-axis are the emissions left uncaptured, stemming either from the steam boiler, associated with electricity consumption or left uncaptured in the flue gas in case of post-combustion capture. The captured emissions are shown in the lower half of the y-axis and are either located in streams of synthesis gas coming from the reformer, or as highly concentrated and therefore captured CO<sub>2</sub> streams. The first bar represents the modeled conventional cracker furnace with  $0.7 \text{ kg}_{\text{CO}_2}/\text{kg}_{\text{Ethylene}}$  emitted to the atmosphere. To its right is the estimate of post-combustion capture added to the conventional cracker model, where 90 % of emissions are captured in a concentrated CO<sub>2</sub> stream. The impact of the steam boiler can be clearly seen here, making up the larger share of uncaptured emissions. The *Hydrogen Firing* scenario stands out, as it has the smallest total bar height and therefore overall emissions. This is due to the smaller (1/3) fuel gas consumption compared to the other scenarios, leading to less carbon being present in the system. While some of the uncaptured emissions are associated with the electricity consumed by the e-SMR and compression, the larger share (3/5) comes from the steam boiler. Both *Oxyfuel*

scenarios have similar total emissions and no steam boiler emissions, but differ in the composition of the captured emissions. For *Oxyfuel V1* the carbon is located in two streams, the reformed and shifted synthesis gas and concentrated stack emissions. *Oxyfuel V2* combines the two streams by re-feeding depleted syngas after hydrogen separation to the cracker furnace for combustion.

As previously, it is worth examining what the emission composition looks like when neglecting the assumption that the net steam generation of the conventional cracker model must be upheld, resulting in Figure 5.5.

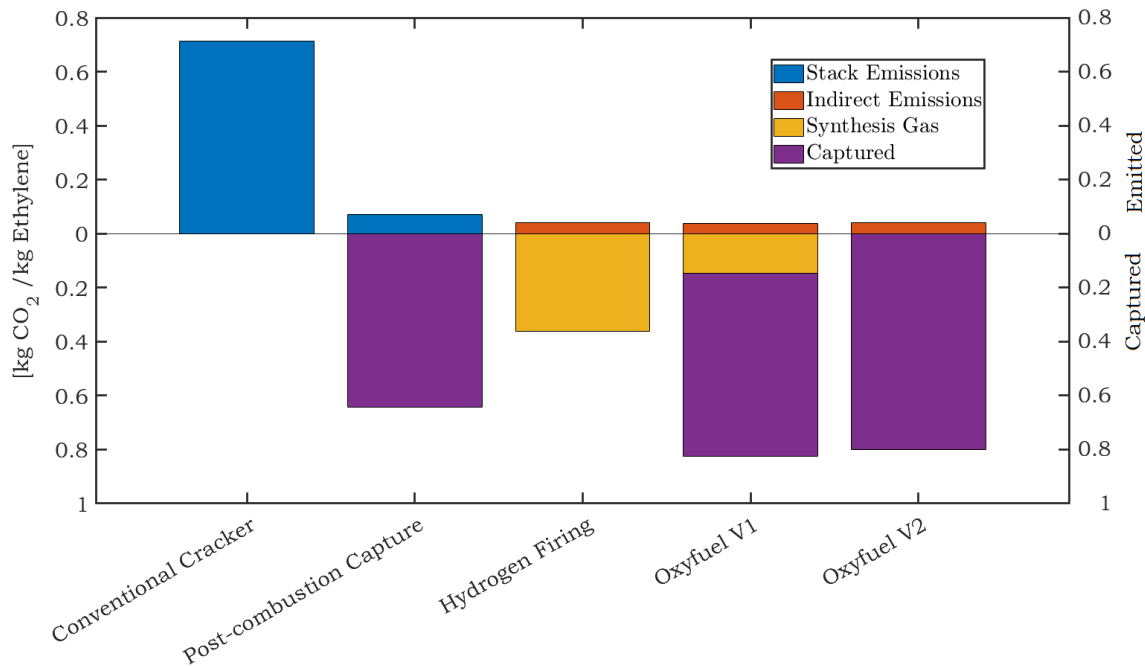


**Figure 5.5:** Emission composition of the investigated scenarios excluding steam generation by a steam boiler

As discussed before, all three integration scenarios end up with a similar flow of uncaptured emissions which are solely indirect emissions associated with electricity. The emission reduction of all scenarios is greater than conventional post-combustion capture by amine absorption, where 10 % of the total emissions are left in the flue gas. Furthermore, the emissions associated with electricity will likely decrease in the future with the expansion of renewable energy generation. The increase in specific energy consumption of the investigated scenarios presented in Figure 5.3 showed that *Hydrogen Firing* and *Oxyfuel V1* require less additional energy input than post-combustion capture, while *Oxyfuel V2* is roughly in the range of post-combustion capture.

Summarizing the findings so far, integration of an e-SMR into an ethane cracker allows significant emission reduction in all three scenarios investigated. The integration of a reformer can have a noticeable impact on steam balance of the cracker furnace. Reforming the methane co-produced during steam cracking of ethane increases specific energy consumption. Depending on the carbon reduction scenario the hydrogen is either combusted or an available output stream.

## 5.4 Carbon Utilization

Figure 5.5 gives an overview of the composition of the captured emissions. This is of special interest when considering the conversion of the captured emissions into products or fuels. As described in Chapter 2.3 there are manifold conversion pathways. This section will provide a first estimate on the potential of the present scenarios to generate olefins from the captured emissions. Hydrogenation of CO and CO<sub>2</sub> to produce methanol, which is converted to olefins amongst other products via MTO is the pathway analysed. The additional energy input required for the carbon utilization is 17.3 MJ/kg<sub>Ethylene</sub> [19].

In the *Hydrogen Firing* scenario, the carbon is isolated in a stream of depleted syngas, which also contains residual hydrogen and some methane. With a H<sub>2</sub>/CO<sub>2</sub> ratio of 0.5 the hydrogen is the limiting factor for synthesizing methanol. For CO<sub>2</sub> hydrogenation typically a ratio of 3 is desired. The potential production of ethylene from the synthesized methanol can increase production capacity by 0.6 %. If additional hydrogen can be supplied by other sources, e.g., by electrolysis of water this potential increases to 4 %.

In the *Oxyfuel* scenarios the emissions are mainly isolated in a pure stream of CO<sub>2</sub>. *Oxyfuel V1* also has a fraction of the emissions present in a stream of shifted syngas. The main difference to the *Hydrogen Firing* scenario is that there is also a stream of pure hydrogen available. For *Oxyfuel V1* the H<sub>2</sub>/CO<sub>2</sub> ratio is 2.2, while it increases to 2.5 for *Oxyfuel V2*. This shows that hydrogen is the limiting factor for the *Oxyfuel* scenarios as well. The respective increase in ethylene yield if this carbon utilization path is pursued is 9.7 % for *Oxyfuel V1* and 13 % for *Oxyfuel V2*.

## 5.5 Discussion

An aspect of the integration of an e-SMR with an ethane cracker that has not been discussed yet is its relation to the ongoing transformation of the industry. The main strategies pursued are replacement of fossil feedstock by recycled waste and biomass. This would impact the investigated scenarios mostly through potential changes to the cracked gas composition. A more important aspect of the steam cracking conversion strategy is the effort to electrify the cracker, eliminating the need to burn fuel to drive the cracking reactions. Evaluating the integration scenarios in this regard requires further analysis, but the significant changes required to operate a cracker furnace with oxy-fuel combustion appear to be opposed to electrifying a cracker, meaning that an investment decision would need to be made between the two options. Partial or complete fuel switching to hydrogen on the other hand seems like an intermediate step in the decarbonization of the industry, as it could be facilitated with relatively small changes to the furnace. Furthermore, the reformation of methane originating the cracking opens several pathways to valorize fuels or additional products from the reformed hydrogen, which is not needed for combustion in the cracker furnace after its electrification.



# 6

## Conclusion

The results presented in this work showed that integration of an e-SMR into an ethane cracker can substantially reduce the emissions associated with producing ethylene. The residual emissions are exclusively associated with the electricity consumed and can therefore be further reduced by increasing the share of renewable electricity production. The performance evaluation of fuel switching to hydrogen combustion depends on assumptions made in regard to the crackers steam balance, as the net steam generation would drop when implementing this scenario according to the models used in this work. If a deficit of steam does not affect operation of the fractionation system of a cracker, fuel switching to hydrogen achieves substantial emission reduction with the lowest increase in specific energy consumption. If the steam deficit has to be substituted by means of a steam boiler running on natural gas, the emissions reduction will be smaller, but still significant, while the specific energy consumption will further increase. The oxy-fuel combustion scenario was analyzed in two different configurations, one including re-feeding depleted syngas originating from reformation and one producing synthesis gas as an output stream. The emission reduction potential is significant in both cases and reaches the same level as hydrogen firing if its steam deficit is not compensated. Regarding the increased energy consumption, the configuration with depleted syngas re-feeding has a higher energy penalty than the other configuration without re-feeding.

An estimate on the potential to produce ethylene from the captured carbon via CO<sub>2</sub> hydrogenation to methanol with subsequent methanol to olefin conversion showed that the specific ethylene production of an ethane cracker can be increased by roughly 9-13 % for oxy-fuel combustion, where hydrogen from reformation is available. In case that emissions are reduced by fuel switching to hydrogen, the increase in specific production is limited to 0.6 % by a deficit of hydrogen. If additional hydrogen can be supplied by other sources, the specific production potential could be increased by 4 %. It should be noted that these values are an estimate and come with an energy input of 17.3 MJ/kg<sub>Olefin</sub>, excluding potential hydrogen production. Nevertheless, the utilization of captured carbon is an interesting strategy to replace some fraction of the fossil feedstock of a cracker plant and allows production of a multitude of products and fuels depending on the conversion pathway chosen.

Further techno-economic assessment of the investigated scenarios and carbon utilization is needed, also considering the synergies within a cracker plant that typically consist of several furnaces, often operating on different feedstock.

## 6.1 Limitations and Suggestions for Future Work

While this work gives a good overview on different emissions reduction measures for a ethane cracker, the impact of integrating a electrified steam reformer and potential carbon utilization pathways, it does not allow recommendation of one of the investigated scenarios. Further techno-economic assessment is needed, which also considers the availability and operational reliability of the technology presented. Furthermore, analysing a stand-alone ethane cracker brings up the issue of external fuel gas supply, as ethane crackers are not self-sufficient when combusting the fuel grade by-products contained in the cracked gas. The inclusion of a potential fuel gas supply in the system boundary increases the complexity of a uniform comparison because the input values may vary. In a similar manner the steam balance of a cracker furnace and the fractionation system adds complexity to the definition of the system boundary and energy analyses. These issues represent the complexity of a cracker plant, but can pose a challenge to modeling.

The inclusion of additional steam crackers running on other feedstock such as naphtha into the analyses, would decrease external inputs, as naphtha crackers typically overproduce combustible gases which are partially used to power other energy consumers of a cracker plant. Unfortunately, this would further increase complexity of the analyses, but would give a more detailed representation of the synergies within a cracker plant and the economic optimization potential.

# Bibliography

- [1] *Steam Cracker*. [Online]. Available: <https://www.schmidt-clemens.com/products/steam-cracker>.
- [2] K. Weissermel and H.-J. Arpe, *Industrial Organic Chemistry*. 2008, ISBN: 3527288384.
- [3] I. Amghizar, L. A. Vandewalle, K. M. Van Geem, and G. B. Marin, “New Trends in Olefin Production,” *Engineering*, vol. 3, no. 2, pp. 171–178, 2017, ISSN: 20958099. DOI: 10.1016/J.ENG.2017.02.006.
- [4] T. Ren, M. Patel, and K. Blok, “Olefins from conventional and heavy feedstocks: Energy use in steam cracking and alternative processes,” *Energy*, vol. 31, no. 4, pp. 425–451, 2006, ISSN: 03605442. DOI: 10.1016/j.energy.2005.04.001.
- [5] M. C. Weigl and G. Schmidt, “Carbon capture in cracking furnace,” in *AIChE 2010 Spring Meeting & 6th Global Congress on Process Safety, San Antonio*, American Institute of Chemical Engineers, 2010.
- [6] C. Oliveira and T. Van Dril, “Decarbonisation options for large volume organic chemicals production, Sabic Geleen,” Tech. Rep., 2021.
- [7] H. Thunman, T. Berdugo Vilches, M. Seemann, *et al.*, “Circular use of plastics-transformation of existing petrochemical clusters into thermochemical recycling plants with 100% plastics recovery,” *Sustainable Materials and Technologies*, vol. 22, 2019, ISSN: 22149937. DOI: 10.1016/j.susmat.2019.e00124.
- [8] C. Mandviwala, “Steam Cracking of Polyolefins in Fluidized Bed Systems: Influences of the Bed Materials on the Hydrogen Transfer Reactions,” 2022.
- [9] O. Mynko, D. J. Brown, L. Chen, *et al.*, “Reducing CO<sub>2</sub> emissions of existing ethylene plants: Evaluation of different revamp strategies to reduce global CO<sub>2</sub> emission by 100 million tonnes,” *Journal of Cleaner Production*, vol. 362, no. May, 2022. DOI: 10.1016/j.jclepro.2022.132127.
- [10] IEA, “Global Hydrogen Review 2021,” *Global Hydrogen Review 2021*, 2021. DOI: 10.1787/39351842-en.
- [11] K. M. Van Geem and B. M. Weckhuysen, “Toward an e-chemistree: Materials for electrification of the chemical industry,” *MRS Bulletin*, vol. 46, no. 12, pp. 1187–1196, 2021, ISSN: 08837694. DOI: 10.1557/s43577-021-00247-5.
- [12] S. T. Wismann, J. S. Engbaek, S. B. Vendelbo, *et al.*, “Electrified methane reforming: A compact approach to greener industrial hydrogen production,” *Science*, pp. 756–759, 2019. [Online]. Available: <http://science.sciencemag.org/>.

- [13] H. Zimmermann and R. Walzi, "Ethylene," in *Ullmann's Encyclopedia of Industrial Chemistry*, vol. 8, 2013, pp. 1–58. DOI: 10.1002/14356007.a10045.pub2.
- [14] J. L. Pellegrino, "Energy and Environmental Profile of the U.S. Chemical industry," Tech. Rep., 2000. DOI: <https://doi.org/10.2172/1218625>.
- [15] European IPPC Bureau, *Best Available Techniques (BAT) Reference Document for the Production of Large Volume Organic Chemicals*. 2017, ISBN: 978-92-79-76589-6. [Online]. Available: [http://eippcb.jrc.ec.europa.eu/reference/BREF/PP\\_BREF\\_FD\\_07\\_2013.pdf](http://eippcb.jrc.ec.europa.eu/reference/BREF/PP_BREF_FD_07_2013.pdf).
- [16] N. S. Sifat and Y. Haseli, "A Critical Review of CO<sub>2</sub> Capture Technologies and Prospects for Clean Power generation," *Energies*, vol. 12, no. 21, p. 4143, 2019, ISSN: 19961073. DOI: 10.3390/en12214143.
- [17] C. Fu and T. Gundersen, "Using exergy analysis to reduce power consumption in air separation units for oxy-combustion processes," *Energy*, vol. 44, no. 1, pp. 60–68, 2012, ISSN: 03605442. DOI: 10.1016/j.energy.2012.01.065.
- [18] E. Esposito, L. Dellamuzia, U. Moretti, A. Fuoco, L. Giorno, and J. C. Jansen, "Simultaneous production of biomethane and food grade CO<sub>2</sub> from biogas: An industrial case study," *Energy and Environmental Science*, vol. 12, no. 1, pp. 281–289, 2019, ISSN: 17545706. DOI: 10.1039/c8ee02897d.
- [19] N. Thonemann, S. Stiebel, D. Maga, *et al.*, "Location Planning for the Production of CO<sub>2</sub>-Based Chemicals Using the Example of Olefin Production," *Chemical Engineering and Technology*, vol. 43, no. 3, pp. 502–513, 2020, ISSN: 15214125. DOI: 10.1002/ceat.201900670.
- [20] A. M. Cormos, C. Dinca, L. Petrescu, D. Andreea Chisalita, S. Szima, and C. C. Cormos, "Carbon capture and utilisation technologies applied to energy conversion systems and other energy-intensive industrial applications," *Fuel*, vol. 211, no. October 2017, pp. 883–890, 2018, ISSN: 00162361. DOI: 10.1016/j.fuel.2017.09.104.
- [21] F. Nahra and C. S. Cazin, "Hydrogenation of Carbon Dioxide," *Science of Synthesis*, vol. 2017, no. 5, pp. 289–313, 2017, ISSN: 25667297. DOI: 10.1055/sos-SD-226-00114.
- [22] P. Tian, Y. Wei, M. Ye, and Z. Liu, "Methanol to olefins (MTO): From fundamentals to commercialization," *ACS Catalysis*, vol. 5, no. 3, pp. 1922–1938, 2015, ISSN: 21555435. DOI: 10.1021/acscatal.5b00007.
- [23] T. Capurso, M. Stefanizzi, M. Torresi, and S. M. Camporeale, "Perspective of the role of hydrogen in the 21st century energy transition," *Energy Conversion and Management*, vol. 251, p. 114 898, 2022, ISSN: 01968904. DOI: 10.1016/j.enconman.2021.114898.
- [24] C. S. Hsu and P. R. Robinson, *Springer Handbook of Petroleum Technology*. Springer, 2017.
- [25] D. Stolten and B. Emons, *Hydrogen Science and Engineering*. 2016, p. 1154, ISBN: 9783527322732.
- [26] E. Baraj, K. Ciahotný, and T. Hlinčík, "The water gas shift reaction: Catalysts and reaction mechanism," *Fuel*, vol. 288, p. 119 817, 2021, ISSN: 00162361. DOI: 10.1016/j.fuel.2020.119817.

- [27] Z. Du, C. Liu, J. Zhai, *et al.*, “A review of hydrogen purification technologies for fuel cell vehicles,” *Catalysts*, vol. 11, no. 3, pp. 1–19, 2021, ISSN: 20734344. DOI: 10.3390/catal11030393.
- [28] C. N. Hamelinck and A. P. Faaij, “Future prospects for production of methanol and hydrogen from biomass,” *Journal of Power Sources*, vol. 111, no. 1, pp. 1–22, 2002, ISSN: 03787753. DOI: 10.1016/S0378-7753(02)00220-3.
- [29] H. Song, Y. Liu, H. Bian, M. Shen, and X. Lin, “Energy, environment, and economic analyses on a novel hydrogen production method by electrified steam methane reforming with renewable energy accommodation,” *Energy Conversion and Management*, vol. 258, p. 115 513, 2022, ISSN: 01968904. DOI: 10.1016/j.enconman.2022.115513.
- [30] D. A. Spagnolo, L. J. Cornett, and K. T. Chuang, “Direct electro-steam reforming: a novel catalytic approach,” vol. 17, no. 11, pp. 839–846, 1992.
- [31] H. Hedström and D. Johansson, “A Pinch Targeting Study of the Borealis Cracker Plant in Stenungsund,” *Chalmers University of Technology*, 2008. [Online]. Available: <https://hdl.handle.net/20.500.12380/68102>.
- [32] IEA, *IEA Energy and Carbon Tracker 2020 - Carbon intensity of industry energy consumption*, 2020. [Online]. Available: <https://www.iea.org/countries/sweden>.
- [33] W. Liemberger, D. Halmschlager, M. Miltner, and M. Harasek, “Efficient extraction of hydrogen transported as co-stream in the natural gas grid – The importance of process design,” *Applied Energy*, vol. 233, pp. 747–763, 2019, ISSN: 03062619. DOI: 10.1016/j.apenergy.2018.10.047.



# A

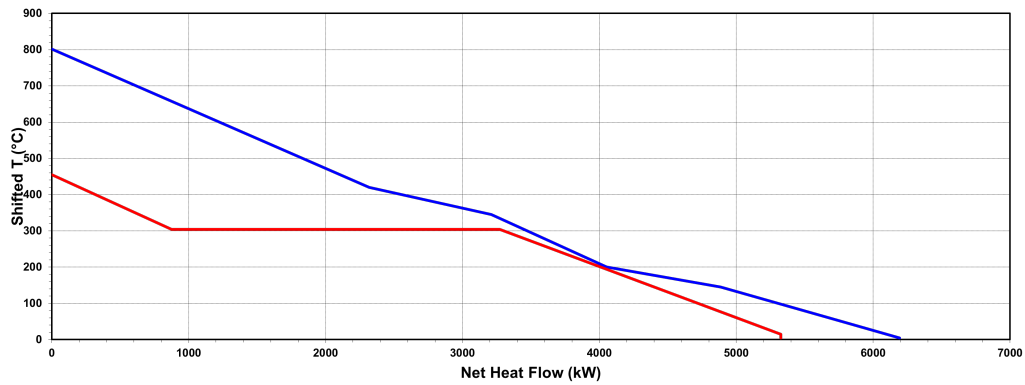
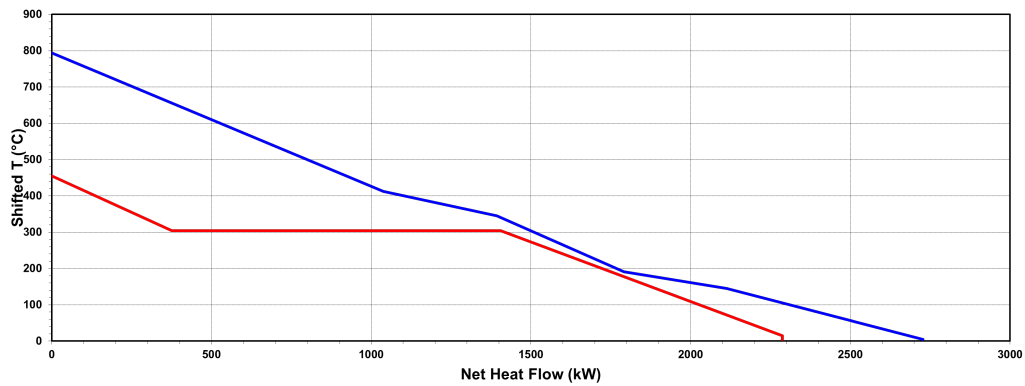
In the reformer model three heat exchangers are used to lower the temperature of the synthesis gas. The first exchangers cools down the synthesis gas coming from the reformer to temperatures favourable for the high-temperature water-gas-shift reactor. Due to the exothermic WGS reaction, the synthesis gas leaves the reactor with an increased temperature and is subsequently cooled by the second heat exchanger. The third heat exchanger cools down the shifted synthesis gas to increase heat recovery. As the steam generation in the convection section of the cracker is in another Aspen hierarchy and integration of the three heat exchangers proved challenging, the process integration tool *Pro-Pi* was used to conduct a pinch analyses. *emphPro-Pi* is a Excel add-in written in Visual Basic. The cooling duty from the three heat exchangers described above is recovered to generate high pressure steam according to the specifications used in this work. The resulting mass flow of steam that can be generated was extracted from *emphPro-Pi*, then normalized to the product of cracking considered in this work, ethylene, and used as additional specific steam generation. The stream data for the two investigated scenarios is shown in a table, while the resulting pinch analyses is presented in two figures. A minimum temperature difference of 10 K was used. The resulting specific steam generation by heat integration of the coolers in the reformer model is  $0.38 \text{ kg}_{steam}/\text{kg}_{Ethylene}$  for Hydrogen Firing and  $0.163 \text{ kg}_{steam}/\text{kg}_{Ethylene}$  for Oxy Fuel.

**Table A.1:** Stream data for the *Hydrogen Firing* scenario

Stream Nr.	Type	$T_{Start}$ in °C	$T_{End}$ in °C	FCp in kW/K	Q in MW
1	Hot	806	350	6.08	2.77
2	Hot	425	150	5.8	1.6
3	Hot	205	20	9.35	1.82
4	Cold	10	299		
5	Cold	299.0	299.1		
6	Cold	299.1	450		

**Table A.2:** Stream data for the *Oxyfuel* scenarios

Stream Nr.	Type	$T_{Start}$ in °C	$T_{End}$ in °C	FCp in kW/K	Q in MW
1	Hot	799	350	2.72	1.219
2	Hot	417	150	2.58	0.69
3	Hot	196	20	4.4	0.82
4	Cold	10	299		
5	Cold	299.0	299.1		
6	Cold	299.1	450		

**Figure A.1:** Heat Integration for *Hydrogen Firing* scenario**Figure A.2:** Heat Integration for *Oxyfuel* scenario

# B

Based on the assumption that the specific net steam generation of the model of a conventional cracker furnace needs to be maintained, a steam boiler running on methane as fuel compensates for steam deficit of the investigated scenarios if necessary. The enthalpy difference of feedwater and superheated steam are extracted from the Aspen model to calculate the energy demand and emissions associated with the steam boiler according to the assumptions below.

Feedwater Temperature	10	°C
Feedwater Pressure	1	bar
Steam Temperature	450	°C
Steam Pressure	85	bar
Enthalpy difference	3.416	MJ/kg <sub>Steam</sub>
Steam Boiler		
Efficiency	90	%
Fuel	Methane	
Specific Emissions	0.055	kg <sub>CO<sub>2</sub></sub> /kJ

B.

---

# C

The user-defined inputs of the Design Specifications used to control the cracker model are shown in the table below.

1 refers to the Design Specification that couples the heat demand/surplus of the two reactors representing the combustion of fuel gas (Gibbs) and cracking of ethane (Yield).

2 refers to the Design Specification used to determine the steam generation by heat recovery in the convection section.

	1	2
Manipulated Stream	Flue Gas	Feed Water
Manipulated Variable	Mass flow	Mass flow
Specification	$Q_{Gibbs}$	$T_{cold-out}$ HX 4 in Figure 4.1
Target Value	$Q_{Yield} * 1.05$	160 °C
Tolerance	10 W	0.1 °C

C.

---

# D

The system boundary for scenario *Oxy V2* is shown in the following table. The difference to *Oxy V1* lays in the re-feeding of depleted synthesis gas to the furnace. Hydrogen is separated from the reformed and shifted synthesis gas by the hybrid separation system consisting of a membrane followed by a PSA, as described in Chapter 4.2.1.

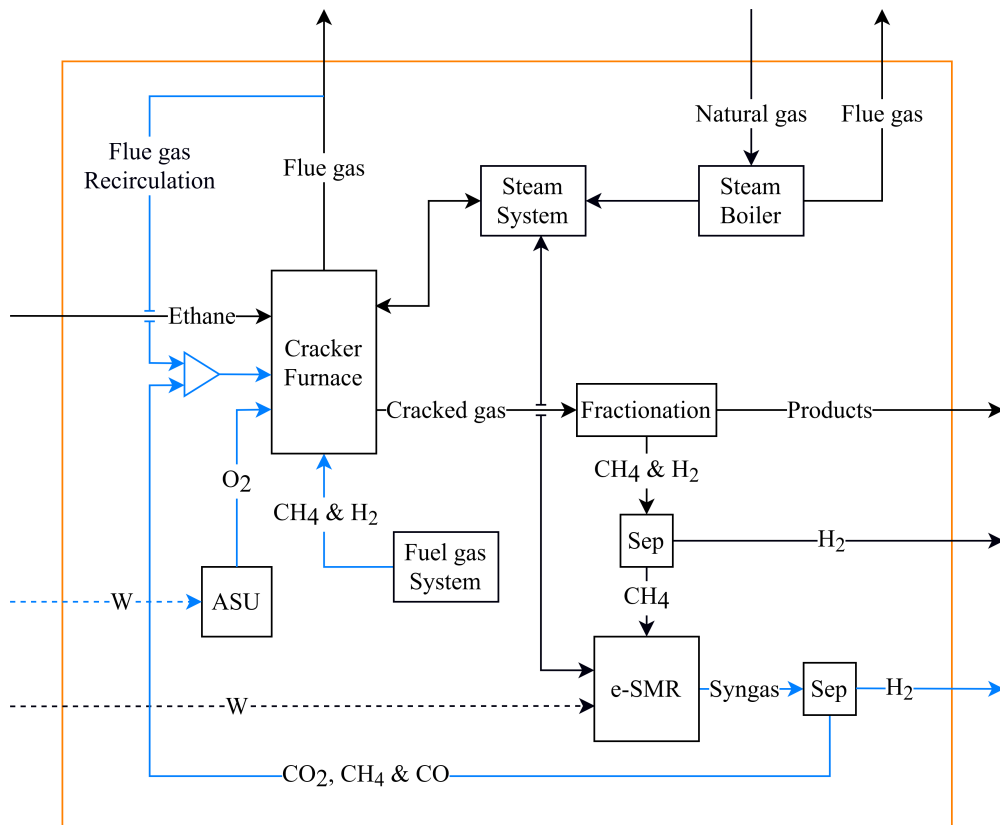


**Figure D.1:** System Boundary for *Oxyfuel V2*

DEPARTMENT OF SOME SUBJECT OR TECHNOLOGY  
CHALMERS UNIVERSITY OF TECHNOLOGY  
Gothenburg, Sweden  
[www.chalmers.se](http://www.chalmers.se)



**CHALMERS**  
UNIVERSITY OF TECHNOLOGY